Particle identification of relativistic heavy ions (II)

Chiara Nociforo

GSI Helmholtzzentrum für Schwerionenforschung
Darmstadt - Germany

IDPASC School – Siena – 2013 Oct 4-6

PID detectors at the Super-FRS

Operation mode with slow-extracted beams

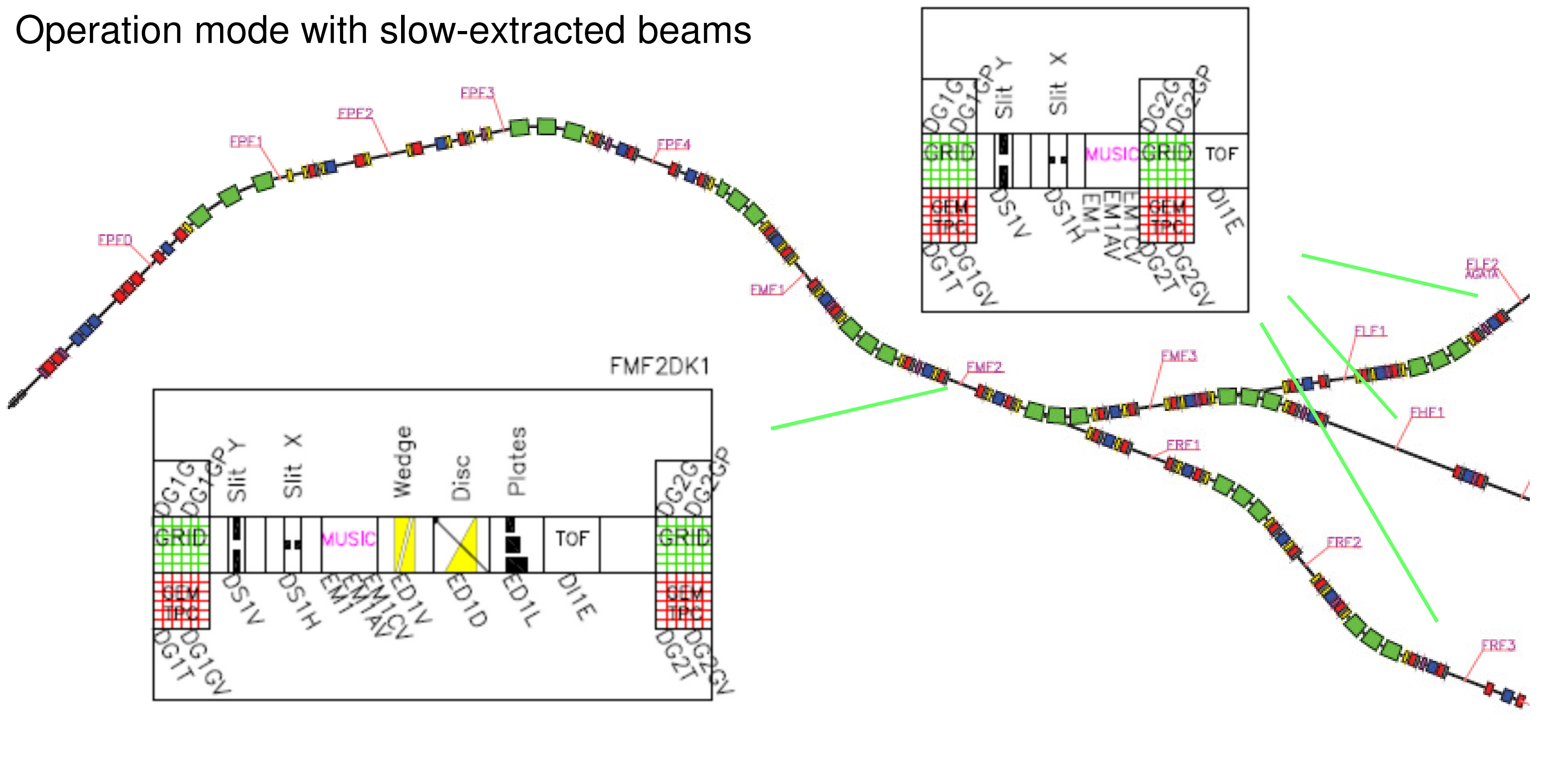

Intensity 10^{12} /s $<10^{10}$ /s $<10^{9}$ /s $<10^{7}$ /s $<10^{5}$ /s

ToF detector

Standard ToF detectors

Nowadays, tracking detectors reach resolution of some tens of μm, then the velocity resolution is limited by the performance of the time measurement, presently of 100 ps (FWHM).

Standard ToF detectors are plastic scintillators read-out by PMTs.

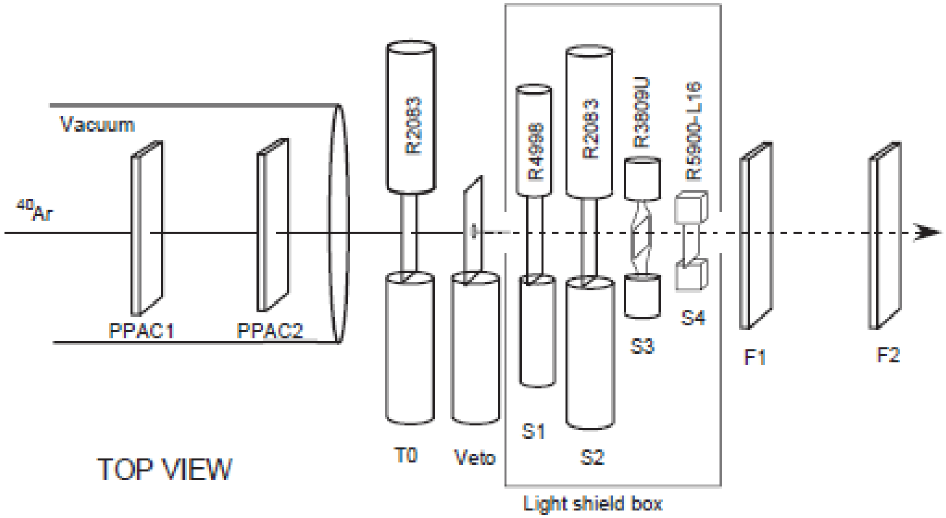

Optimization of scintillation detector for heavy ion beams indicates higher timing resolution scaling by the pulse height and the number of photoelectrons N produced at the photocathode ($\sigma_t \propto 1 / \sqrt{N}$).

S. Nishimura et al., *NIM A* 510 (2003) 377

ps resolution on ^{238}U ToF

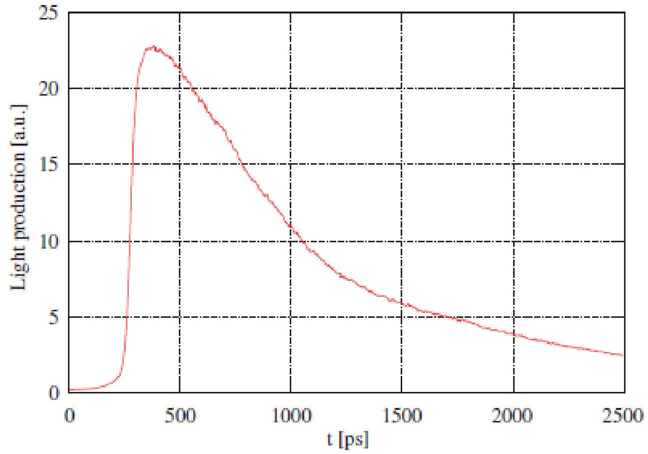

Fig. 5. Typical response from the streak camera. Measured rise-time = 40 ps, decay-time = 550 ps.

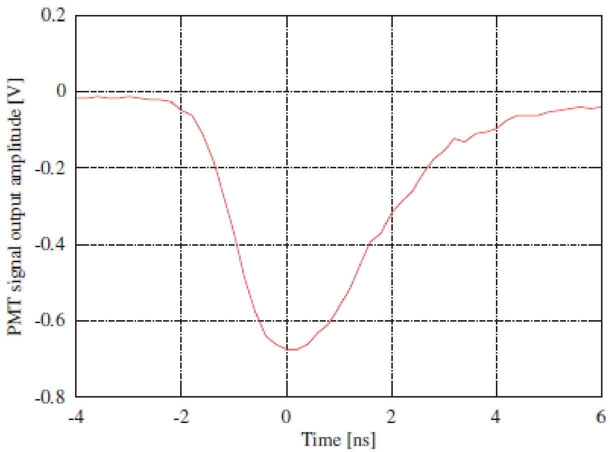

Fig. 6. Example of a PMT output signal waveform.

FWHM= 17 ps

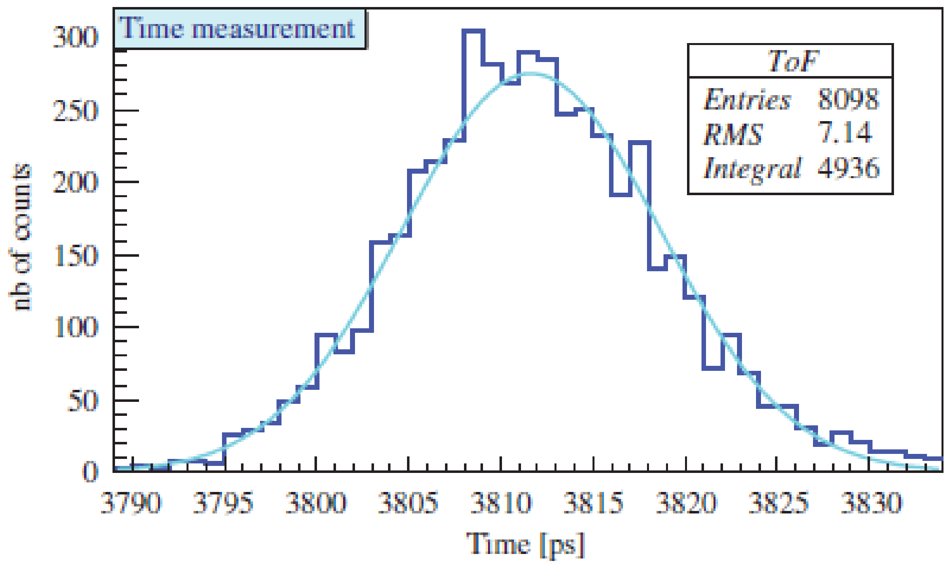

Fig. 13. Time-of-flight measurement at GSI with an ^{238}U beam at 600 A.MeV. Start detector: $150 \times 32 \times 1$ mm^3, Stop detector: $600 \times 32 \times 4$ mm^3. Only H6533 PMTs are used for that measurement.

A. Ebran et al., *NIM A* 728 (2013) 40

Other solutions ?

Radiation hard detector (diamond, silicon)

- 4 units
- time resolution σ <50 ps
- active area 380/200mm x 50mm
- max rate 500 Hz/mm^2
- high precision time distribution and time stamping

pcCVD-DD → (200 x 40) mm^2 , 20 units 20x20x0.3 mm
(~17 euro/mm^2)
50 strips/units , in total 1000 chs
(~50 euro/ch)

- 100 days operation @1MHz: 1.08×10^{11} ions/cm^2

Absorbed dose = 4.36×10^5 Gy (^{238}U@350 MeV/u)

Characteristics diamond vs silicon

- Wider bandgap energy
  cooling not needed
- Larger carrier mobility
  stronger E field
- Fast signal collection
  typical rise-time ~ 100 ps
- Radiation hardness and no doping
- Low noise (in principle)
  low dielectric constant (ε_r=5.7) – low capacitance
  small leakage current – low noise

	Silicon	Diamond
Bandgap Energy E_g(eV)	1.13	5.47
e-h Prod. Energy(eV)	3.6	12.84
e^- Mobility(cm^2/Vs)	1500	2200
h^+ Mobility(cm^2/Vs)	600	1600
Breakdown Volt.(V/cm)	3×10^5	10^7

Radiation hardness study with Au beam - amplitude reduction

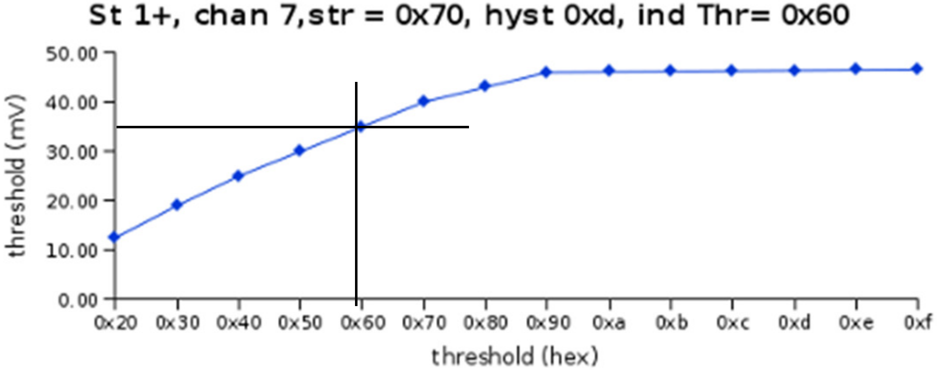

Threshold characteristics (Aug11): cut amplitudes lower than 35mV

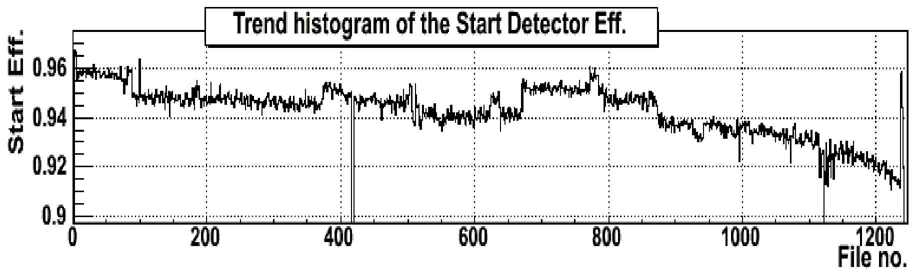

+ 30 % DAQ off + 30 % beam times in 2010

→ 3.04 x 10^{11} Au ions / mm^2

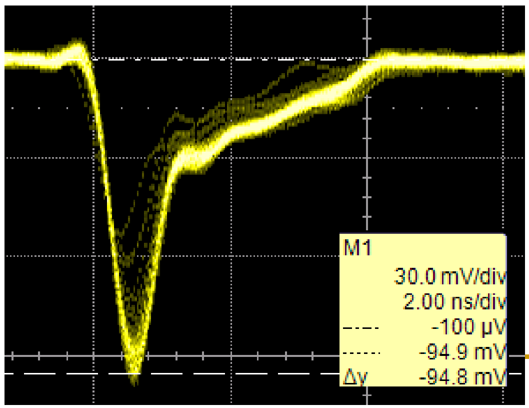

Analog signals, Au beam, HV: 100V
Amplitude; 94 mV

- ➔ After 3.04 x 10^{11} Au ions /mm^2 about 5% of signals below 35 mV
- ➔ Total absorbed dose : 7.9 Grad (312 MeV / Au ion)
- ➔ Amplitude reduction by a factor of 2.7
- ➔ Precise CCE measurment needed

1Grad = 10^7 Gy

Physical parameters of diamond and semiconductors

Table 2.1: Properties of some semiconductor materials that could be used as detector bulk material [Mol06, Owe04a, ioffe]. For the values marked with stars new experimental data and discussion on scCVD diamond are given in this work (see Chapter 6).

property	diamond	silicon	Ge	GaAs	4H-SiC	detector operation
band gap $[eV]$	5.48	1.12	0.67	1.43	3.26	+ high T operation
dielectric strength $[V/cm]$	10^{7*}	3×10^5	10^5	4×10^5	5×10^6	+ high field operation
intrinsic resistivity $[\Omega/cm]$	$>> 10^{11}$	2.3×10^5	50	10^7	$> 10^5$	+ low leakage current
electron mobility $[cm^2/Vs]$	$1900-4500^*$	1350	3900	8000	1000	+ fast signal
hole mobility $[cm^2/Vs]$	$1800-3500^*$	480	1900	400	115	+ fast signal
electron lifetime [s]	$10^{-10}-10^{-6*}$	$> 10^{-3}$	$> 10^{-3}$	10^{-8}	5×10^{-7}	+ full charge collection
hole lifetime [s]	$10^{-10}-10^{-6*}$	10^{-3}	2×10^{-3}	10^{-7}	7×10^{-7}	+ full charge collection
saturation velocity $[cm/s]$	$1.2-2.7\times10^{7*}$	1×10^7	6×10^6	$2-1\times10^7$ [a]	3.3×10^6	+ fast signal
density $[g/cm^3]$	3.52	2.33	5.33	5.32	3.21	
average atomic number	6	14	32	31.5	10	+ therapy - tissue equiv.
dielectric constant	5.72	11.9	16	12.8	9.7	+ low capacitance
displacement energy $[eV]$	43	$13-20$	28	10	$20-35$	+ radiation hardness
thermal conductivity $[Wm^{-1}K^{-1}]$	2000	150	60.2	55	120	+ heat dissipation
energy to create e-h $[eV]$	$11.6-16^*$	3.62	2.96	4.2	7.8	- lower signal
radiation length, X_0 $[cm]$	12.2	9.36	2.3	2.3	8.7	+ low background
Energy loss for MIPs $[MeV/cm]$	4.69	3.21	7.36	5.6	4.32	
Aver. Signal Created / 100 μm	3602	8892	24860	13300	5100	+ lower signal
e-h pairs/X_0 $(10^6 cm^{-1})$	5.7	10	5.67	2.99	4.5	

[a] negative absolute drift velocity

M. Pomorski, *PhD thesis* – Uni Frankfurt (2008)

Absorption spectrum of pure diamond

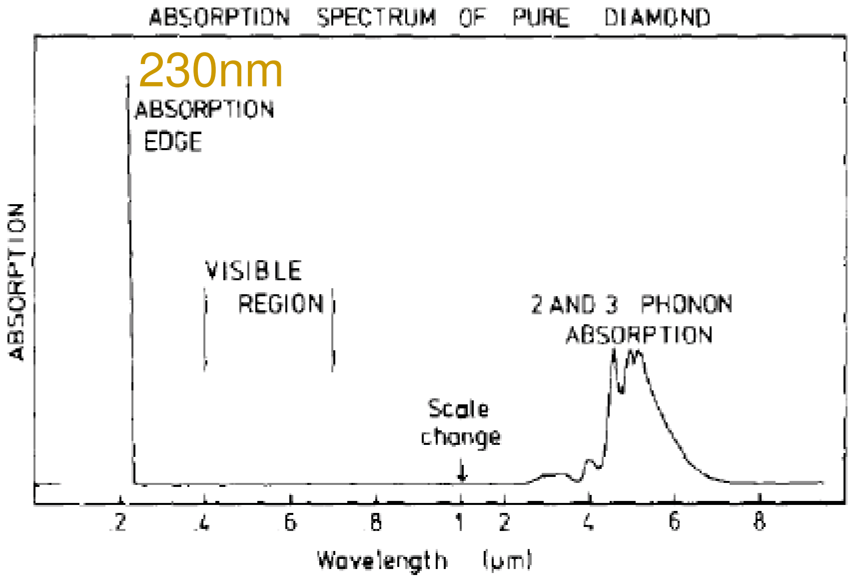

A. T. Collins, *Physica B*, vol. 185, p. 284, 1993

Due to transparency in the Vis range, particle detectors made of high purity diamond are solar-blind.

Some historical background

- The first documented attempt to grow diamond by Chemical Vapor Deposition (CVD) was by G. Eversole of the Union Carbide Corporation (USA) in 1952.

In contrast to the High-Pressure-High-Temperature (HPHT) diamond synthesis process, the CVD method allows to grow diamond of reproducible physics properties in a high purity environment.

- In 1982, a group at the National Institute of Research in Inorganic Materials (NIRIM), Japan, built the first reactor dedicated to diamond growth (10 μm/h).

- The first high quality ´electron grade´ scCVD diamonds were grown by Element Six in 2002 (http://www.e6cvd.com/cvd/page.jsp?pageid=369).

A detailed review of the various methods used for fabricating diamonds can be found in P. W. May, Diamond thin films: a 21st-century material, *Phil. Trans. R. Soc. Lond. A*, vol. 358, p. 473, 2000.

Electronic stopping power in diamond

ρ = 3.52 g/cm^2

ATIMA calculations

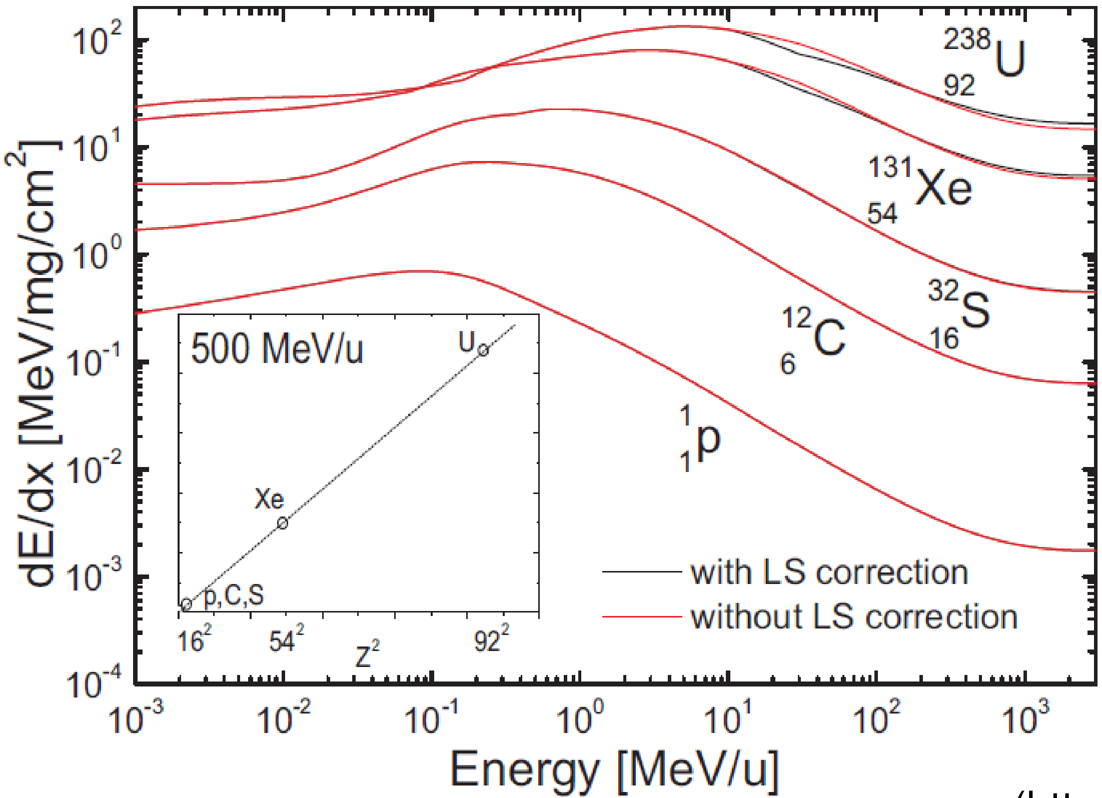

ATIMA code

(http://web-docs.gsi.de/~weick/atima/)

Signal formation

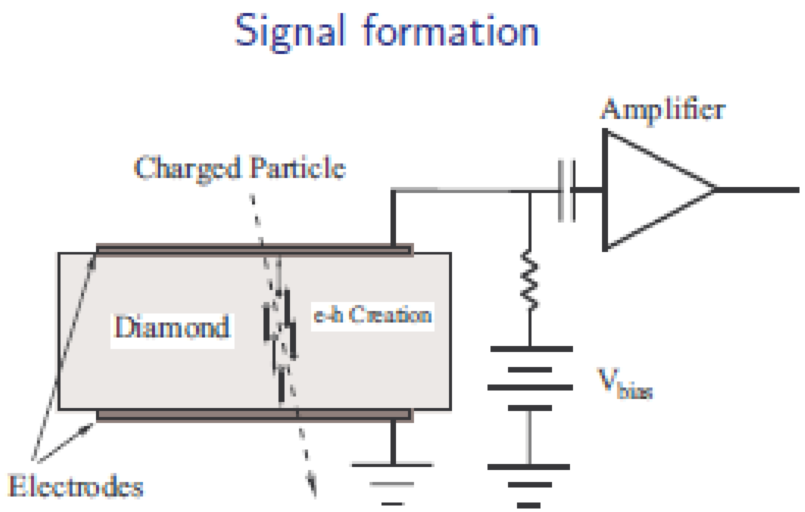

In order to get a signal from the detector, the free charge carriers generated by ionizing particles have to move towards the collecting electrodes. Thus the detector has to be metallized from two sides to apply a voltage and create an electric field, to force the electrons and holes to drift through the detector. The contacts have to be done in such a way that no free charge carriers can enter the diamond from the metal (non-injecting contacts) when a bias voltage is applied, but at the same time, excess charge carriers must be efficiently extracted from the diamond bulk.

^{241}Am source pulse

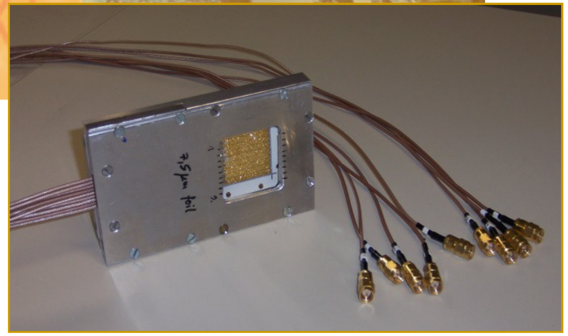

9 strips pcCVD -DD

(30x30) mm^2 , 360 μm thickness, 9 strips (3 mm each)

C=10 pF/strip

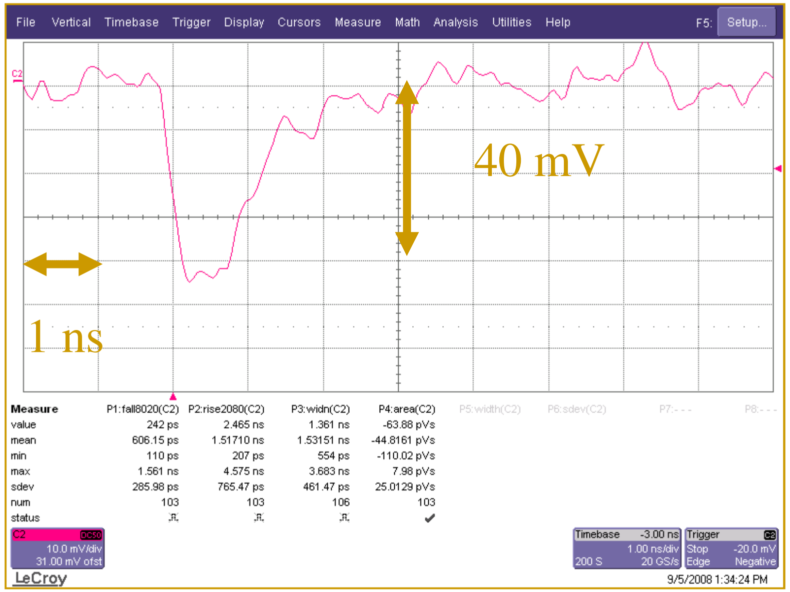

strip #7 -400V

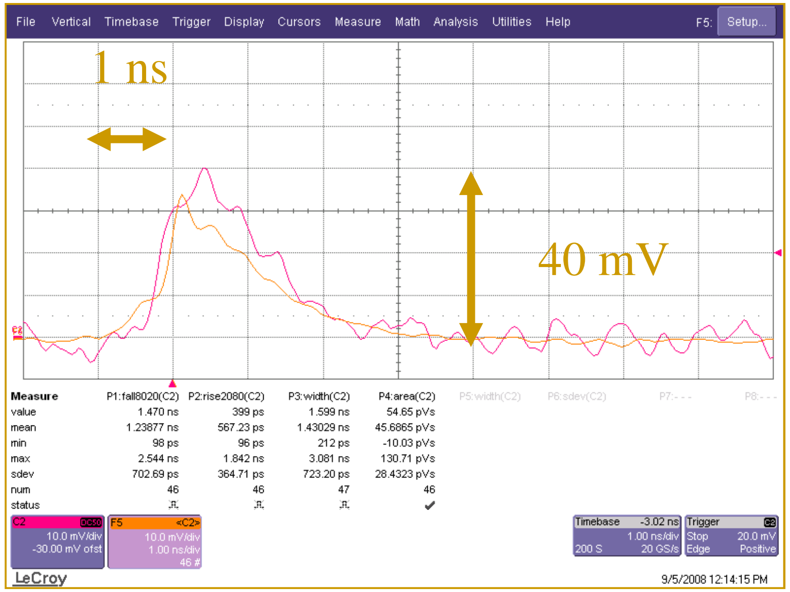

strip #6 +300V

Diamond time properties

^{238}U @350MeV/u

pcCVD -DD **10x10x0.2 1 mm³**

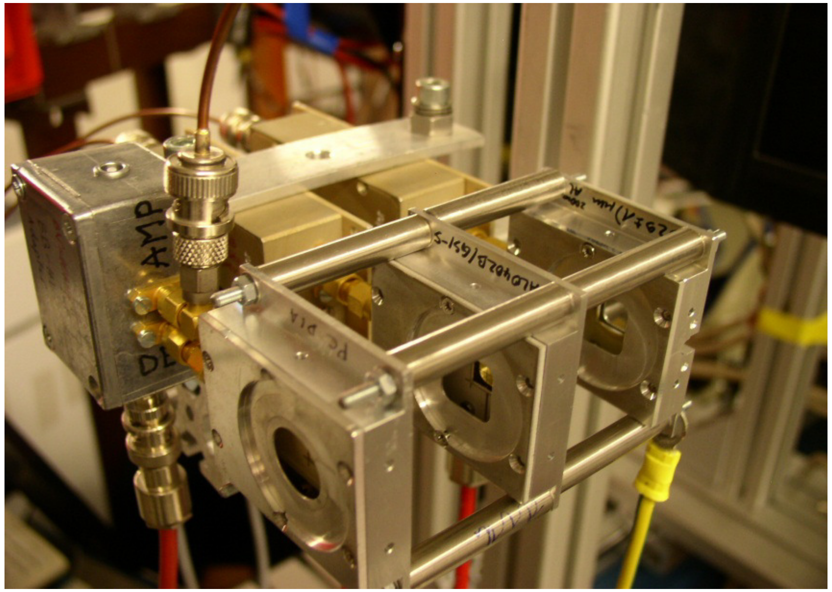

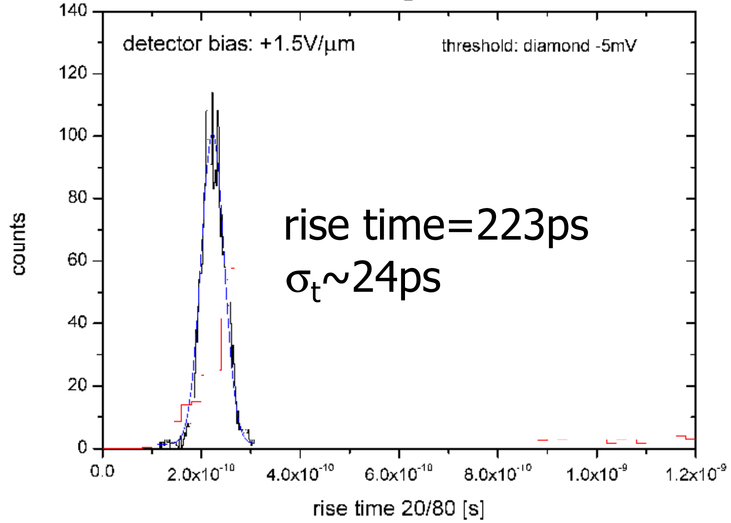

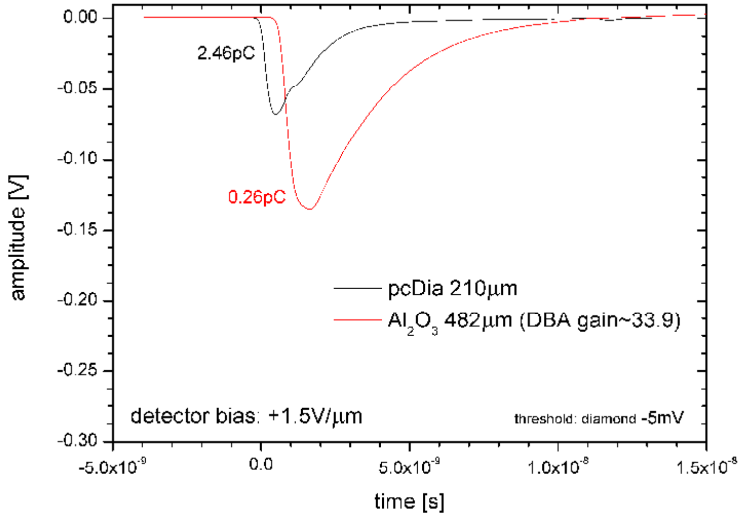

- digital waveform sampled (20 GS/s scope)
- small charge collection Q=2.46pC

GSI-DL
GSI-FRS

Silicon time properties

^{197}Au @750MeV/u

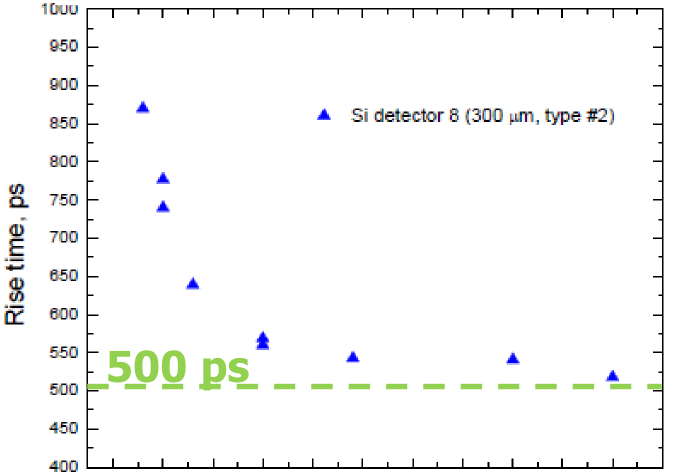

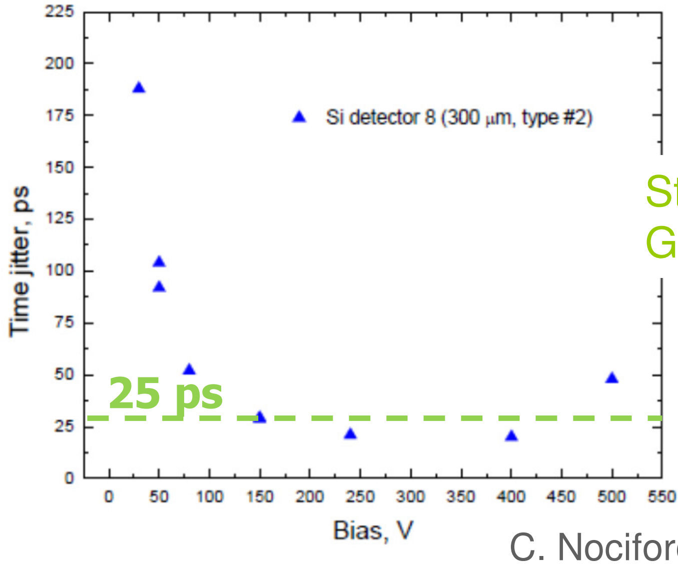

- matched to Si-strip capacity
  (ρ= 10 kOhm cm)
- digital waveform sampled
  (2GHz bandwidth scope)
- time jitter ~ 20ps

Si samples

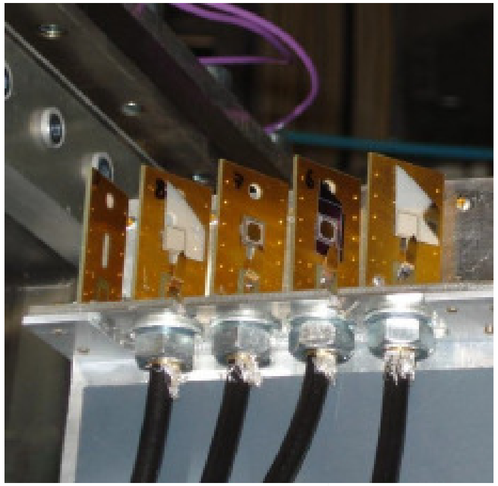

St. Petersburg,
GSI-FRS

^{238}U @350MeV/u

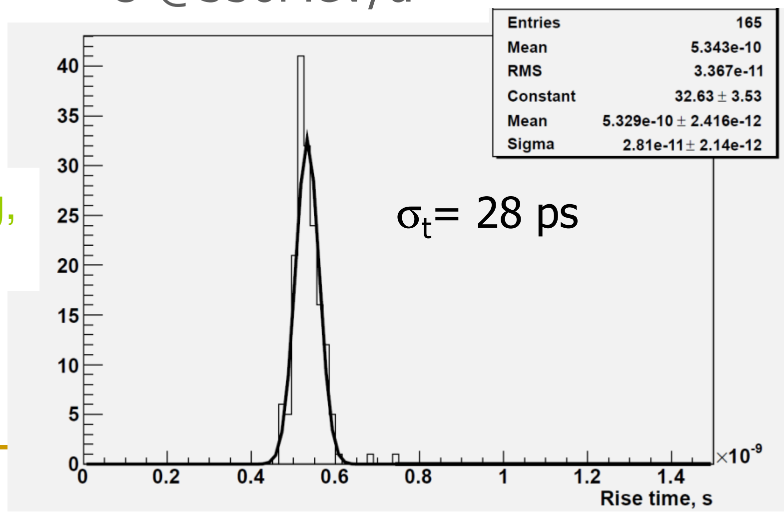

Time resolution (jitter)

$$\sigma_j = \frac{\sigma_e}{(dV/dt)_{threshold}}$$

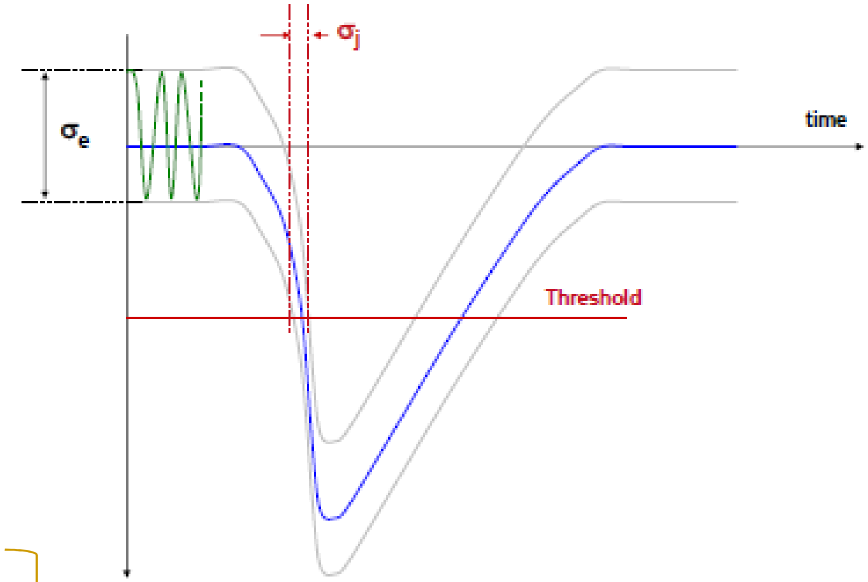

- Increasing signal-to-noise ratio
- Decreasing rise time
- Decreasing jitter

improves time resolution

It is preferable to preserve the fastest possible rise time and use sufficiently broadband readout electronics.

Time over Threshold technique

Time precision is given by the time jitter

$$\sigma_t = \frac{\sigma_n}{\left(\frac{dV}{dt}\right)_{V_T}} + \delta t$$

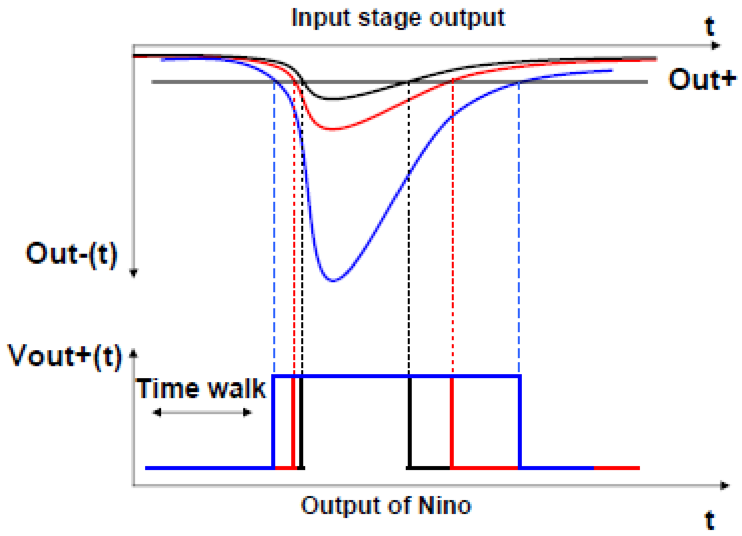

ToT in NINO/PADI chip

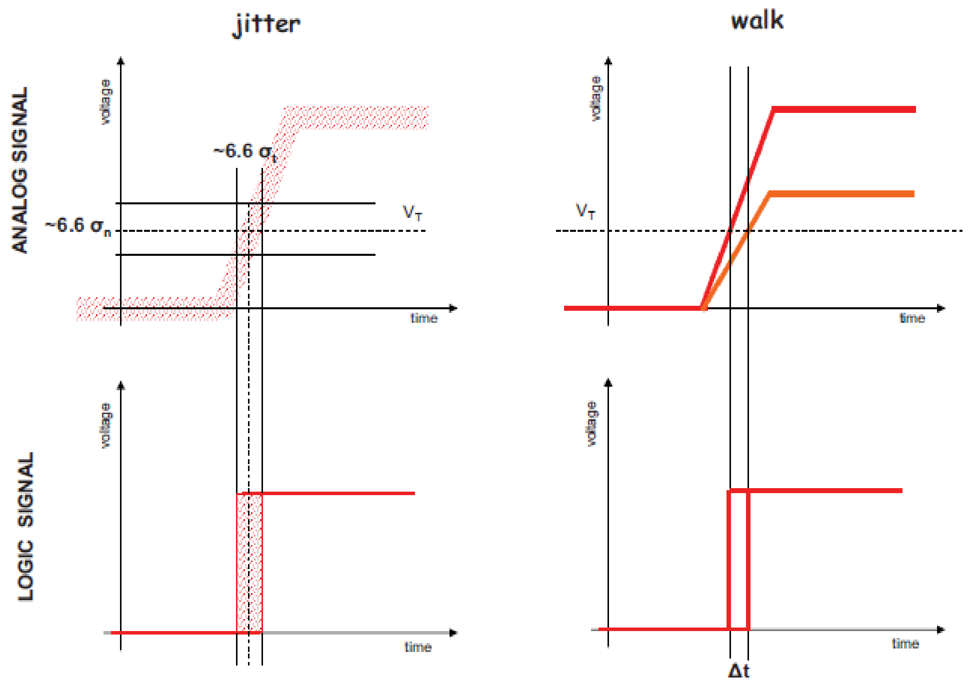

Electronics with ToT capability

- **PADI4** ASIC 0.18 μm CMOS
  - rise time < 500 ps
  - 30 fC <Q< 2000 fC
  - σ_{tE} < 15 ps
  - LVDS digital outputs
  - 350 MHz bandwidth

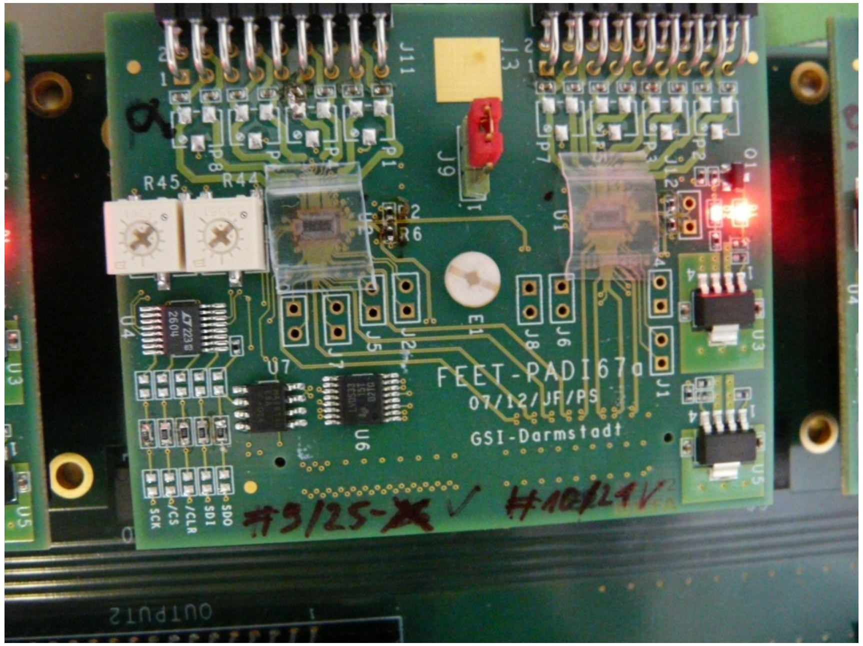

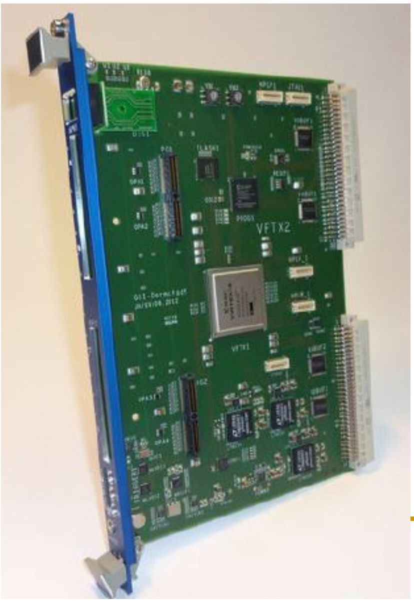

- **VFTX** (28 chs) VME FPGA TDC
  - LVDS inputs
  - 200 MHz clock (internal or external)
  - σ_t < 10 ps

GSI-DL
GSI-EE

VFTX + PADI results

LED

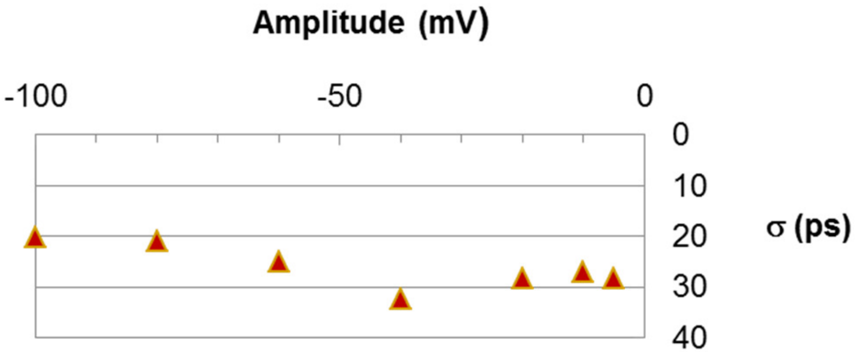

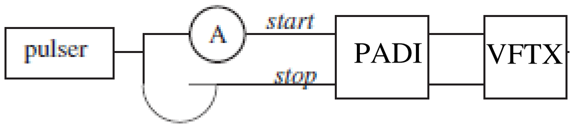

ToT

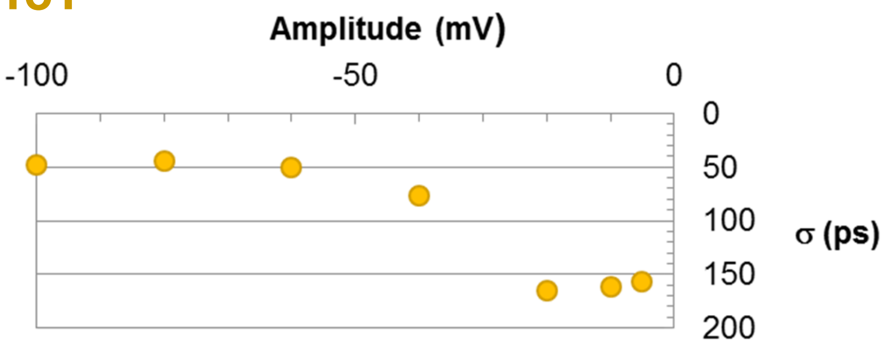

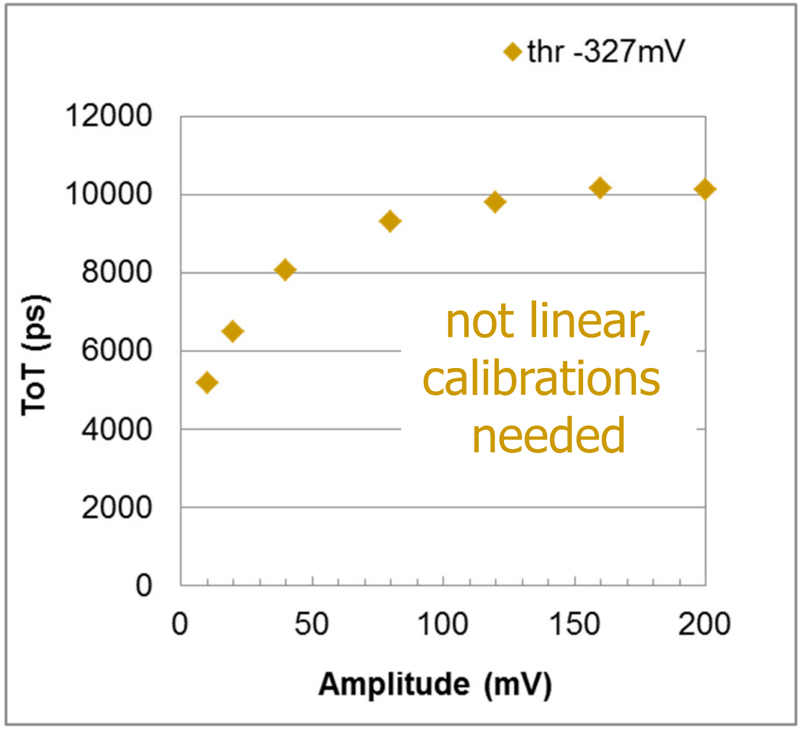

Timing measurements with CVD-DD

$\sigma_{intr} = \sigma_{ToF}/\sqrt{2} = \sqrt{((\sigma_{start}^2 + \sigma_{stop}^2)/2)}$

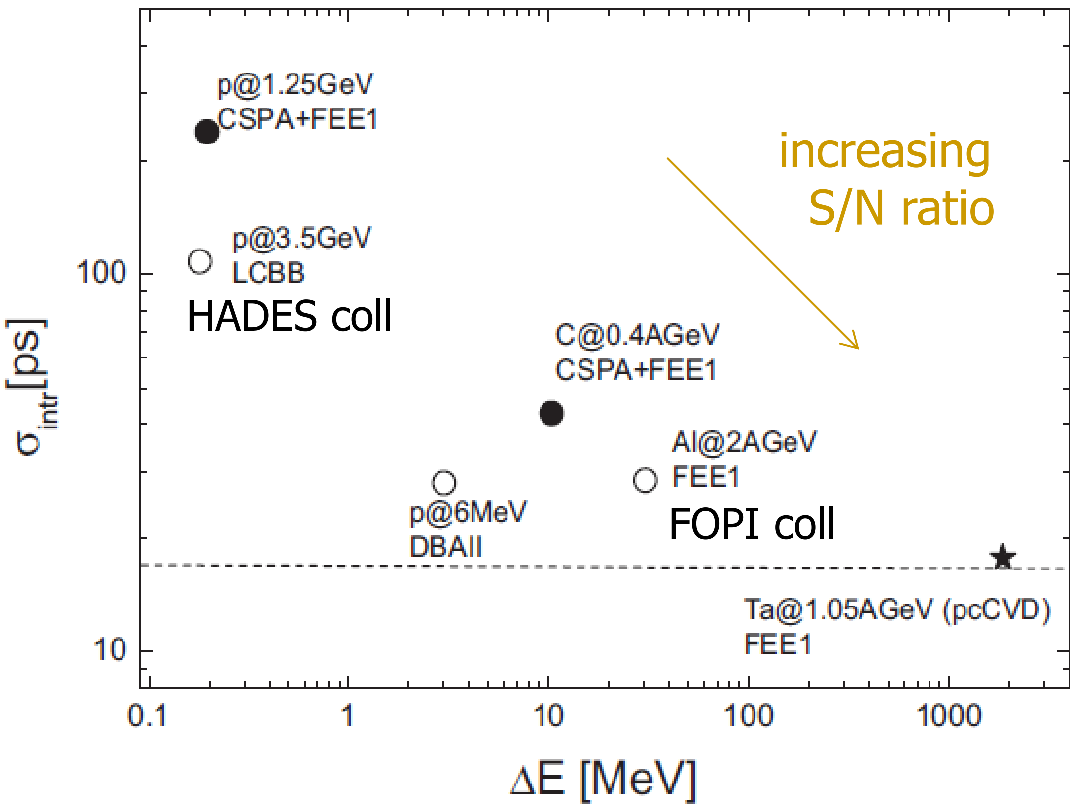

M. Pomorski, *PhD thesis* – Uni Frankfurt (2008)

Prototype design

pcCVD -DD **20x20x0.3 mm^3**

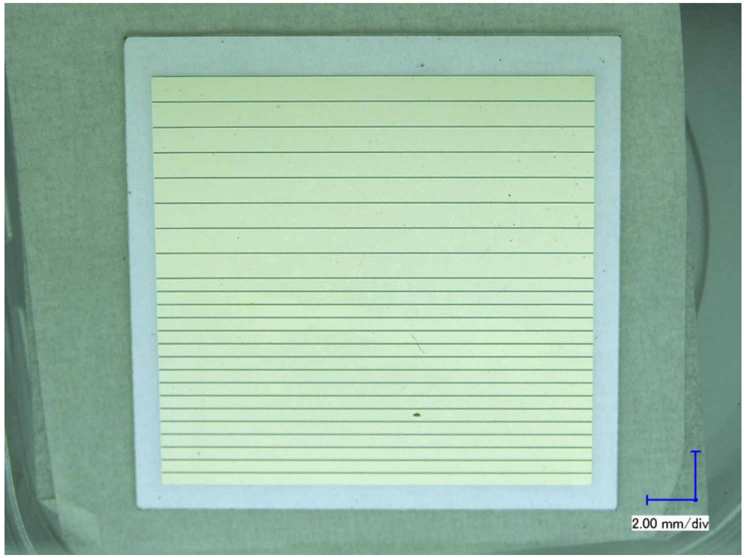

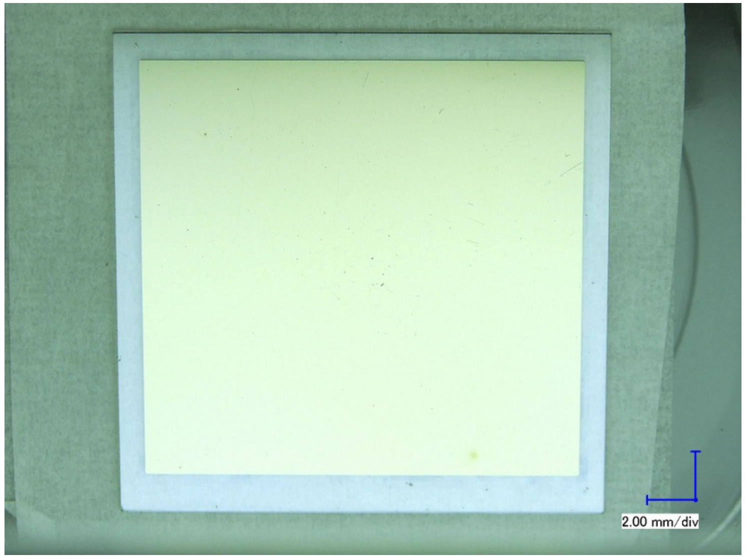

- Electrode metallization with Cr/Au with thickness 50/100 nm
- Photolithography by laser followed by etching
- 8 strips (1 mm) + 16 strips (0.5 mm) – Gap 60 μm
- Annealing of the device at 500º in Ar

GSI-DL

Tracking detector

Time Projection Chamber (TPC)

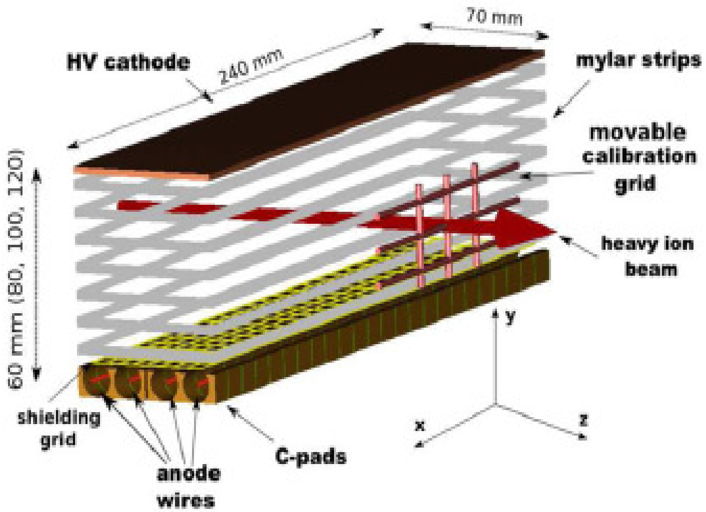

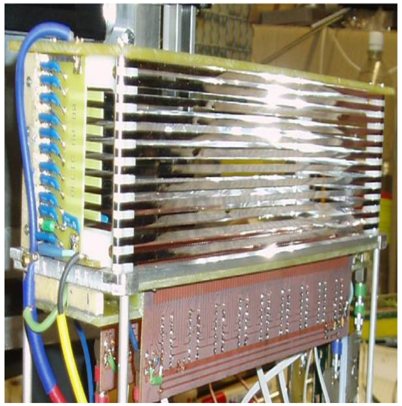

CUB
GSI-FRS

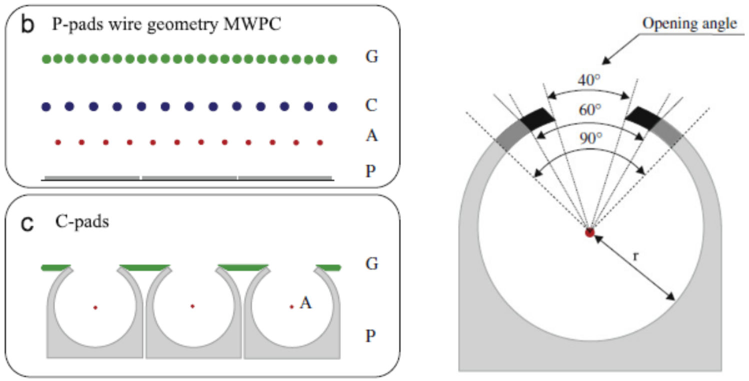

- gas P10 at 1 atm
- integrated delay lines (2x-pos, 4y-pos)
- σ_x ~ 0.1 mm, σ_y~ 0.05 mm
- 95% efficiency at ~100kHz

In operation as standard FRS det since 2005.

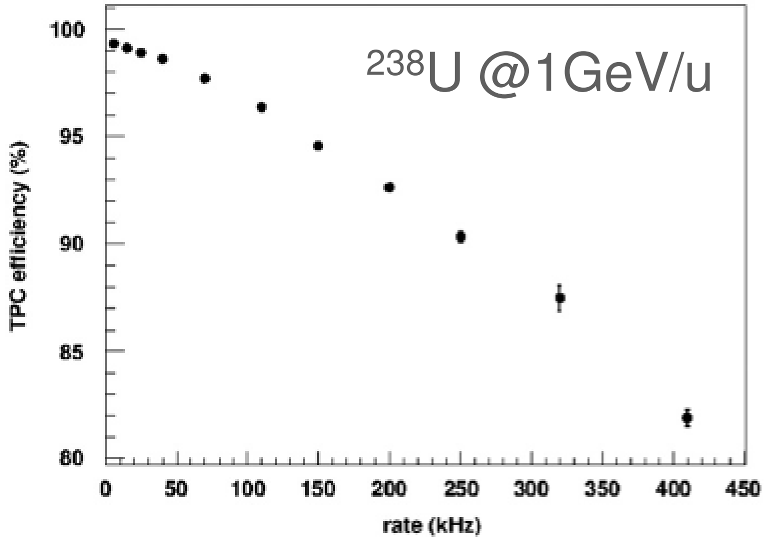

R. Janik et al., *NIM A* 640 (2011) 54

^{24}O study

PRL 102, 152501 (2009) PHYSICAL REVIEW LETTERS week ending 17 APRIL 2009

One-Neutron Removal Measurement Reveals ^{24}O as a New Doubly Magic Nucleus

R. Kanungo,[1,*] C. Nociforo,[2] A. Prochazka,[2,3] T. Aumann,[2] D. Boutin,[3] D. Cortina-Gil,[4] B. Davids,[5] M. Diakaki,[6] F. Farinon,[2,3] H. Geissel,[2] R. Gernhäuser,[7] J. Gerl,[2] R. Janik,[8] B. Jonson,[9] B. Kindler,[2] R. Knöbel,[2,3] R. Krücken,[7] M. Lantz,[9] H. Lenske,[3] Y. Litvinov,[2] B. Lommel,[2] K. Mahata,[2] P. Maierbeck,[7] A. Musumarra,[10,11] T. Nilsson,[9] T. Otsuka,[12] C. Perro,[1] C. Scheidenberger,[2] B. Sitar,[8] P. Strmen,[8] B. Sun,[2] I. Szarka,[8] I. Tanihata,[13] Y. Utsuno,[14] H. Weick,[2] and M. Winkler[2]

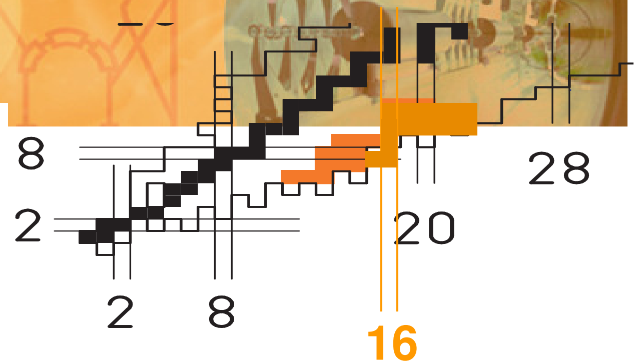

FRagment Separator (FRS)

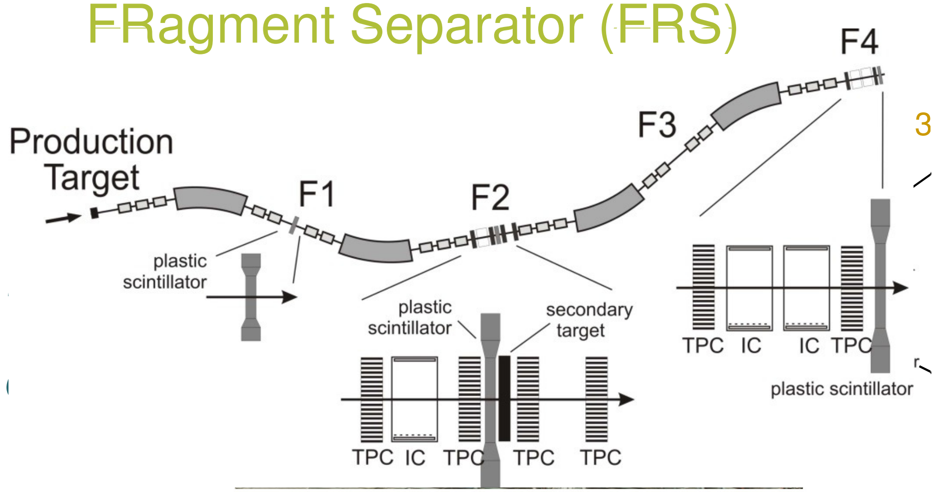

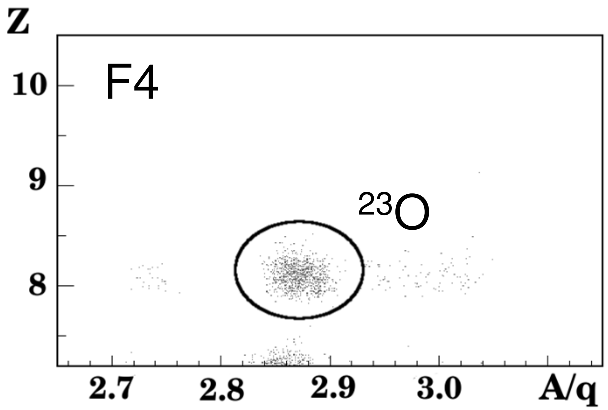

node "

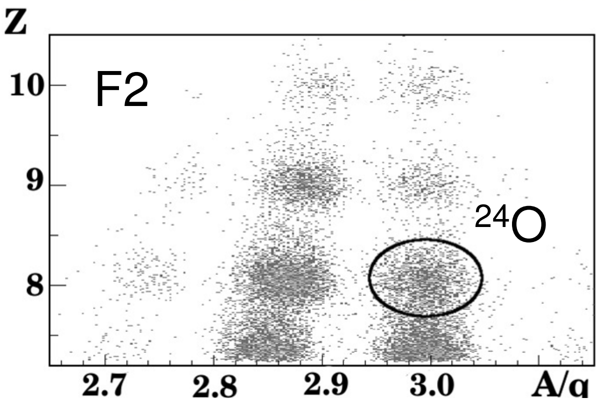

High-resolution momentum (~$1.5\cdot10^{-4}$) in 1*n* removal channel

$$P_f^{lab} = (1 + \frac{x_4 - M x_2}{D_{24}}) z_f B\rho$$

N=16 magic number and shell gap

In the c.m. frame: $P_{||} = \gamma_b (P_f^{lab} - \beta_b E_f^{lab})$

^{24}O: 1*n* removal reaction @920 MeV/u

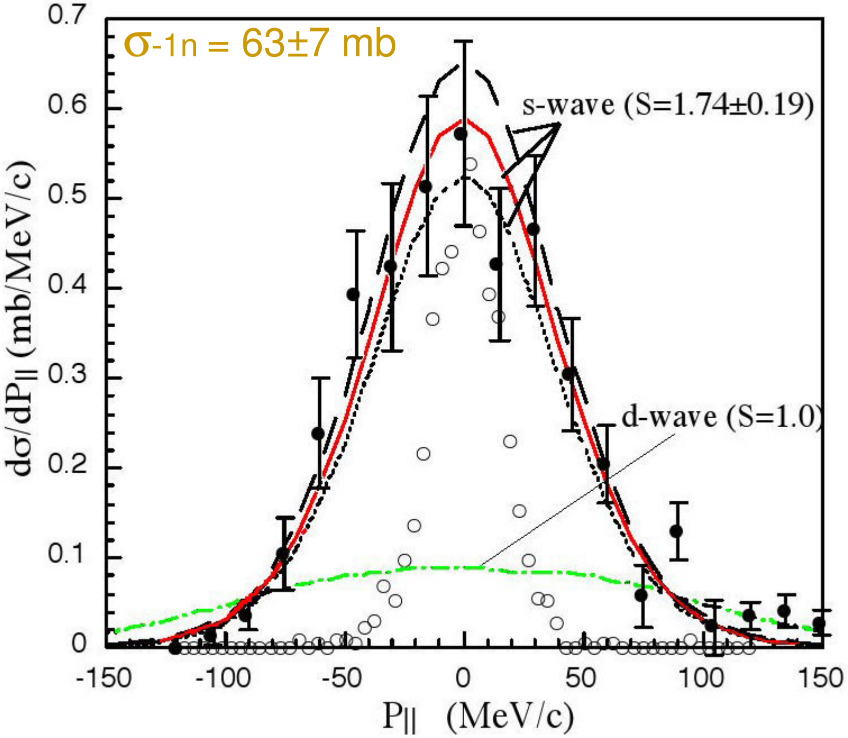

^{23}O states

Spin	SDPF-M Energy(MeV)	SDPF-M C^2S	USDB Energy(MeV)	USDB C^2S	Exp S
$1/2^+$	0.0	1.769	0.0	1.810	1.74(19)
$5/2^+$	2.586	5.593	2.593	5.665	
$3/2^+$	4.736	0.065	4.001	0.090	

... in agreement with shell model calculations

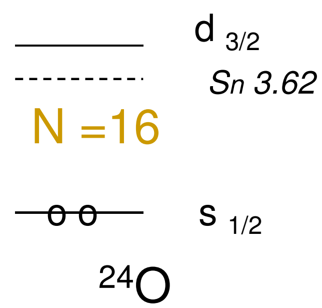

s-wave dominance indicates the presence of a new shell closure at N=16 in ^{24}O

FAIR GEM-TPC detector

Finnish in-kind contribution to FAIR is fixed to 32 GEM-TPC detectors for Super-FRS beam diagnoses and tracking

GEM-TPC detector R&D is currently ongoing at Helsinki / HIP together with GSI, University of Jyväskylä and CUB Bratislava.

Previously, three prototypes have been completed and successfully tested at GSI / FRS beam line.

Currently, GEMEX board- based on n–XYTER chip- is being designed and tested, and a new twin GEM-TPC prototype, i.e. GEM-TPC detector with two field cages in one housing box, is being constructed.

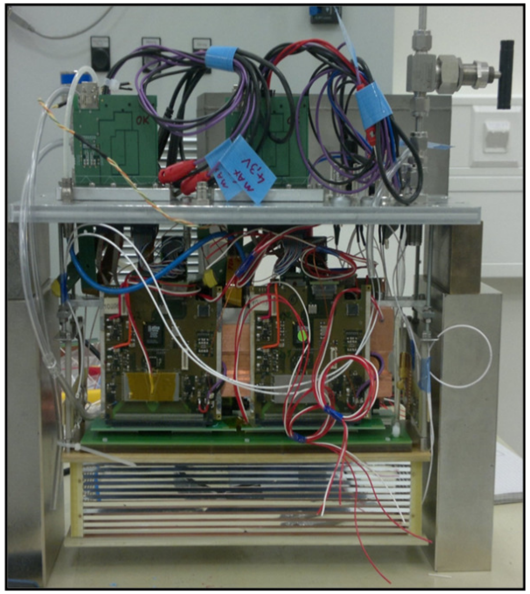

HB3 (Helsinki-Bratislava-#3) GEM-TPC prototype with GEMEX readout cards incl. nXYTER chip

Triple GEM detector

Gas Electron Multiplier

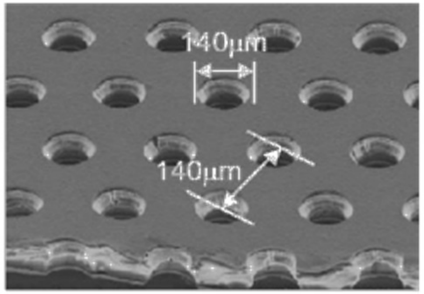

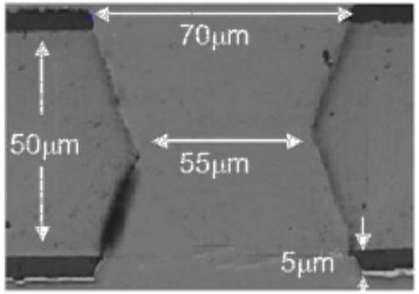

http://gdd.web.cern.ch/GDD/

F. Sauli, *NIM A* 386 (1997) 531

at the Super-FRS the drift will be 80 mm !

Three foils configuration advantages:

- reduced discharge probability (i.e. higher gains achievable)
- ion feedback effects suppression

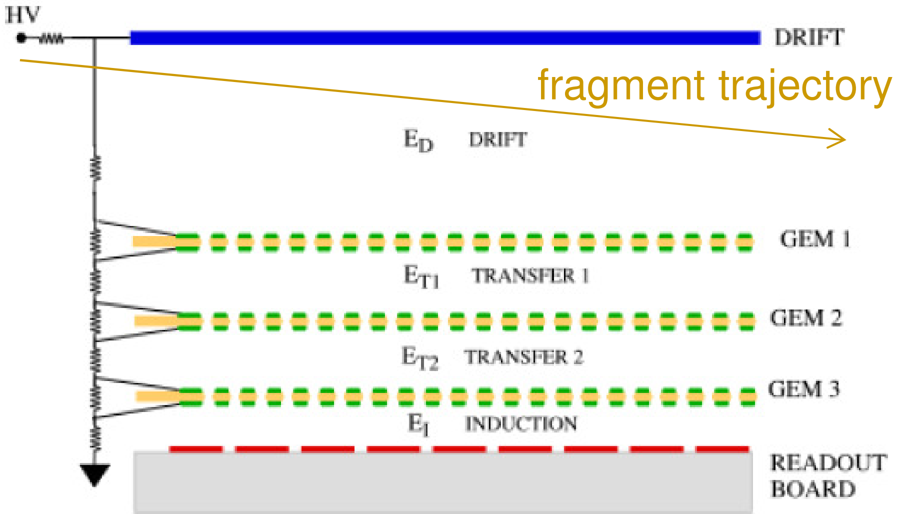

HB3 GEM-TPC prototype

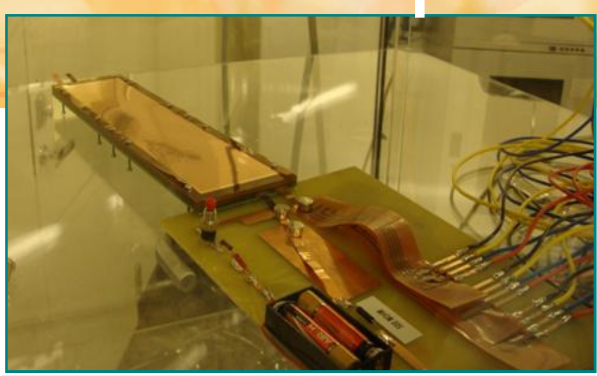

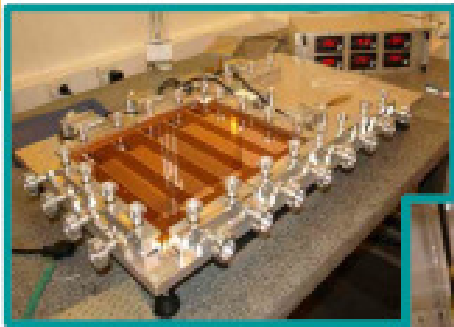

GEM foil Framing - Frascati stretcher

HELSINKI INSTITUTE OF PHYSICS

Triple GEM stack

GEM foil - Leakage Current measurement

GSI

GEMEX card with two n-xyters

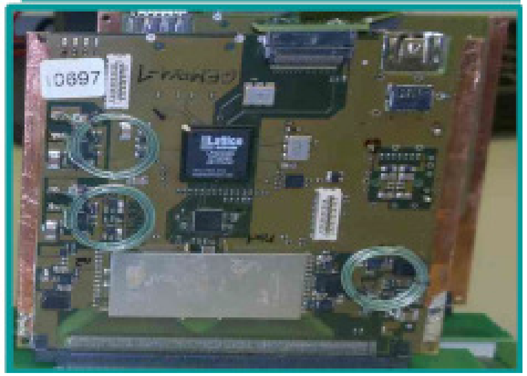

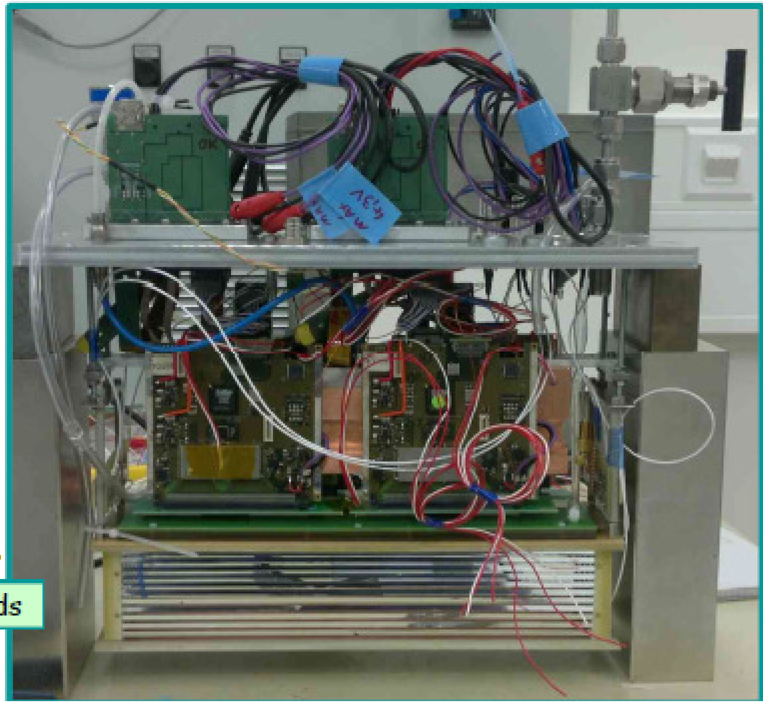

HB3 with four GEMEX cards

n-XYTER functional principles

128 ch, asynchronous channel trigger
for the (self-triggered) detection of statistical, Poisson distributed signals

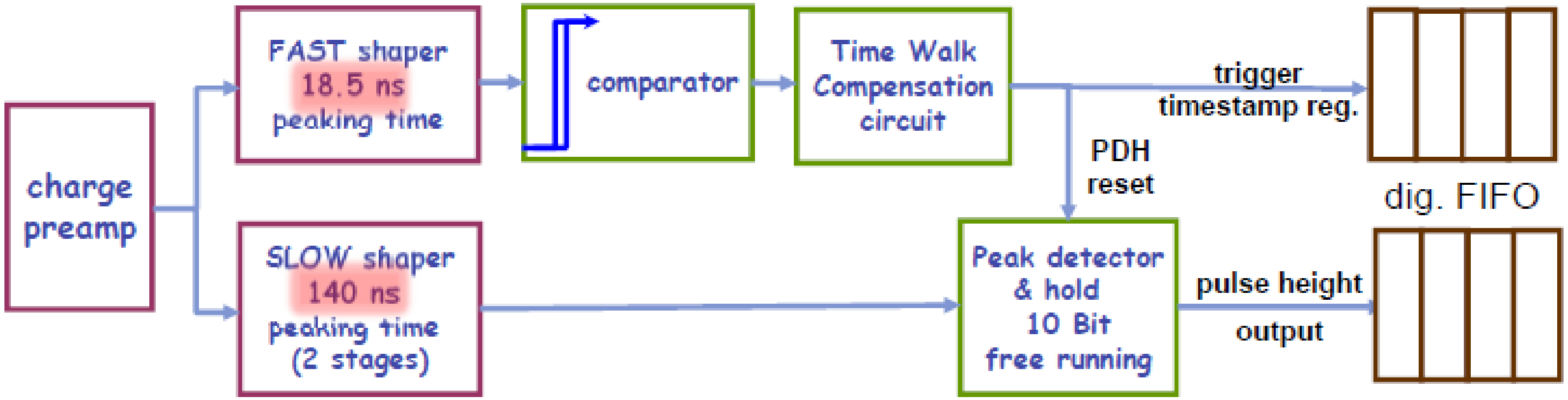

i.e. practically dead time free for the envisaged 1-10 MHz particle rate !

Asynchronous registry and storage
in 4-level FIFO guarantees data loss <4 %
when read-out through balancing token ring
with 32 MHz data registry and read-out

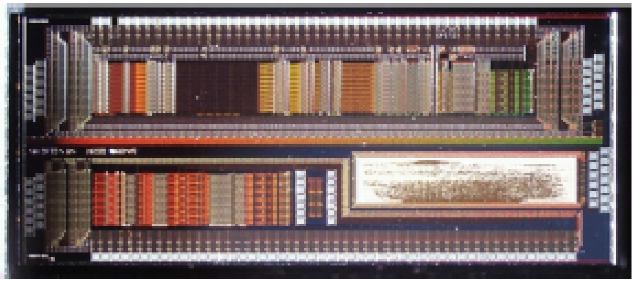

DETNI XYTER ASIC 1.0, in AMS 0.35μ

GEMEX

GEMEX Gas-Electron-Multiplier EXploder system GSI

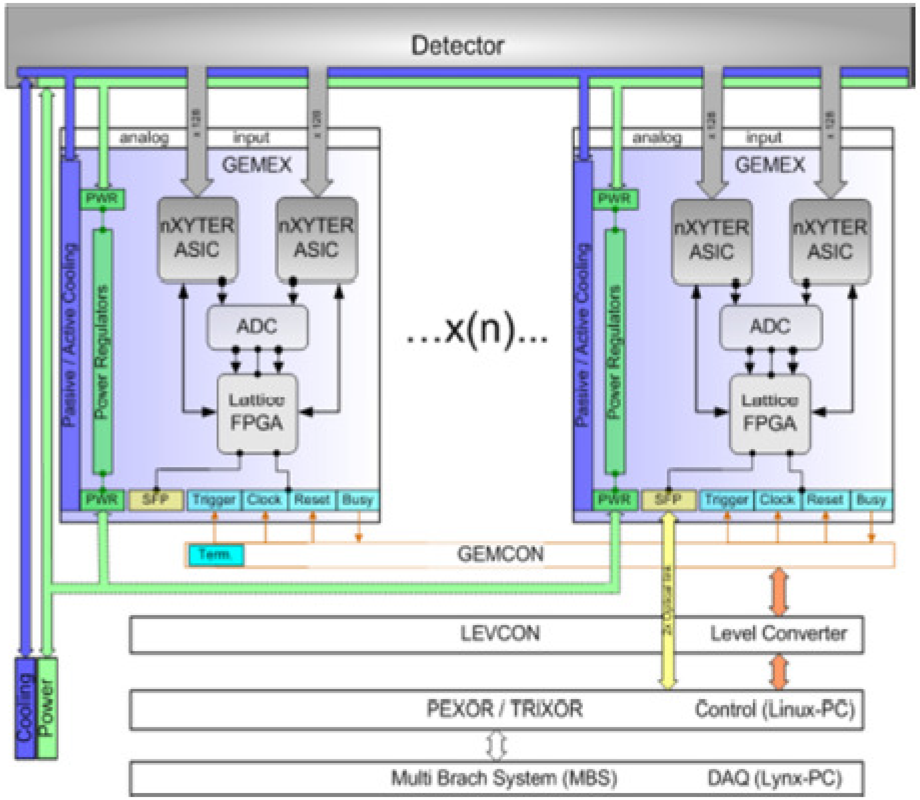

- Two nXYTER ASICs
- 256ch/card, 6.3V@2.1A
- Pipelining 12 Bit ADC, sampling rate 32 Ms/s (2ch)
- Dyn.range 600e$^-$..120ke$^-$ **too small !**
- Synchronized trigger & time-stamping logic, high precision PLL synthesizer

Test results of HB1

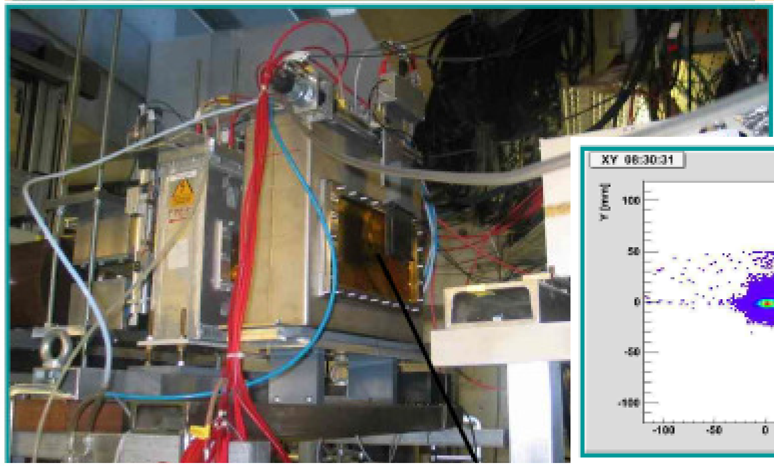

First GEM beam test at the FRS !

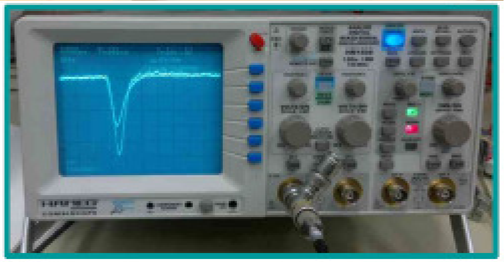

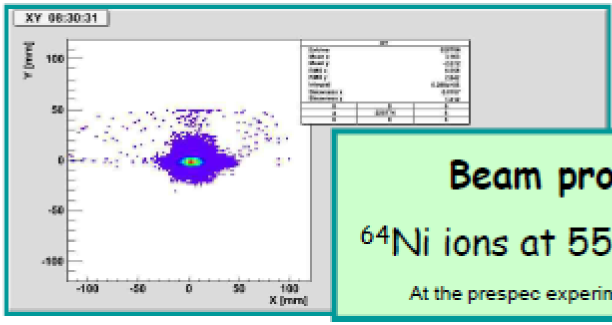

Beam profile

^{64}Ni ions at 550 MeV/u

At the prespec experiment - S363

HIP
CUB
GSI

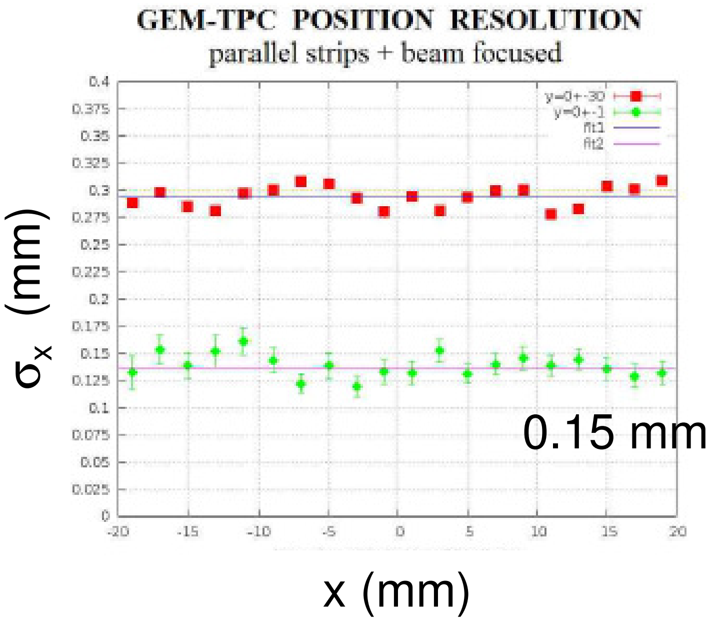

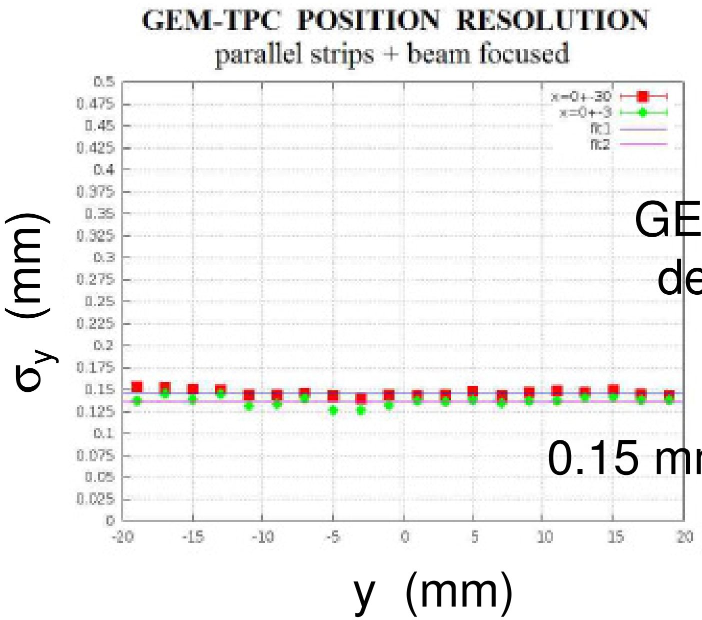

GEM foils + delay lines

Test results of HB3

HB3 @ S2 and ready to take the Beam of ^{197}Au at 770 MeV/u

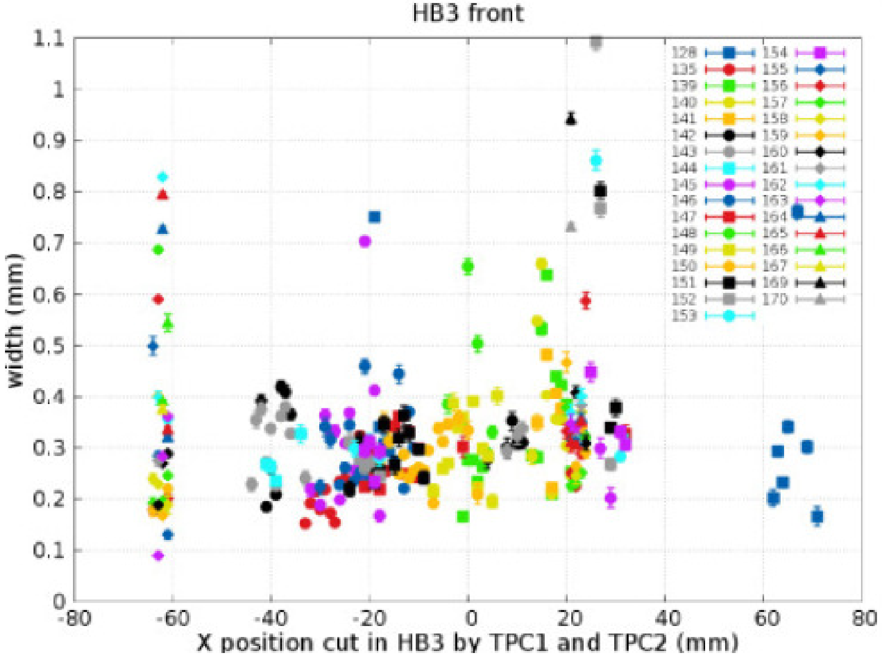

GEM +
GEMEX

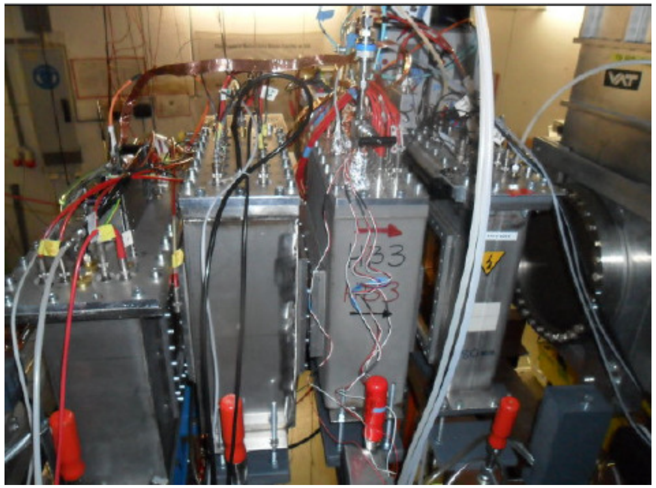

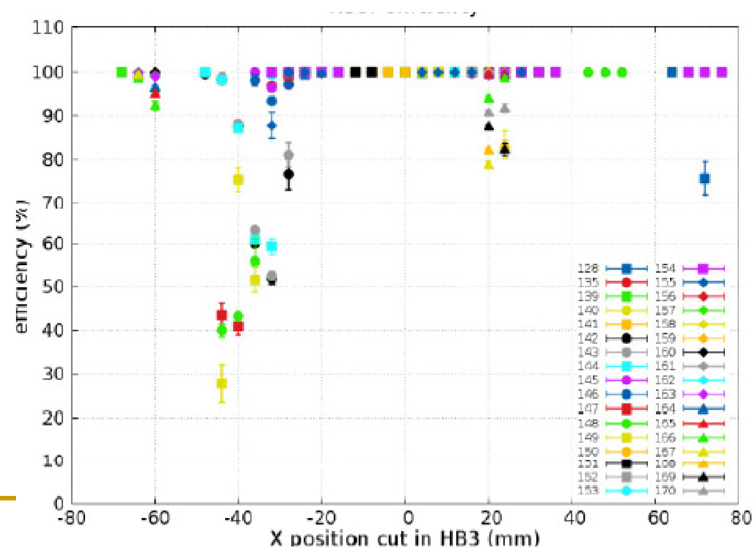

HIP
CUB
GSI

High-rate solution

Simulations

- trigger window <2 μs
- hit mixing starts @750 kHz

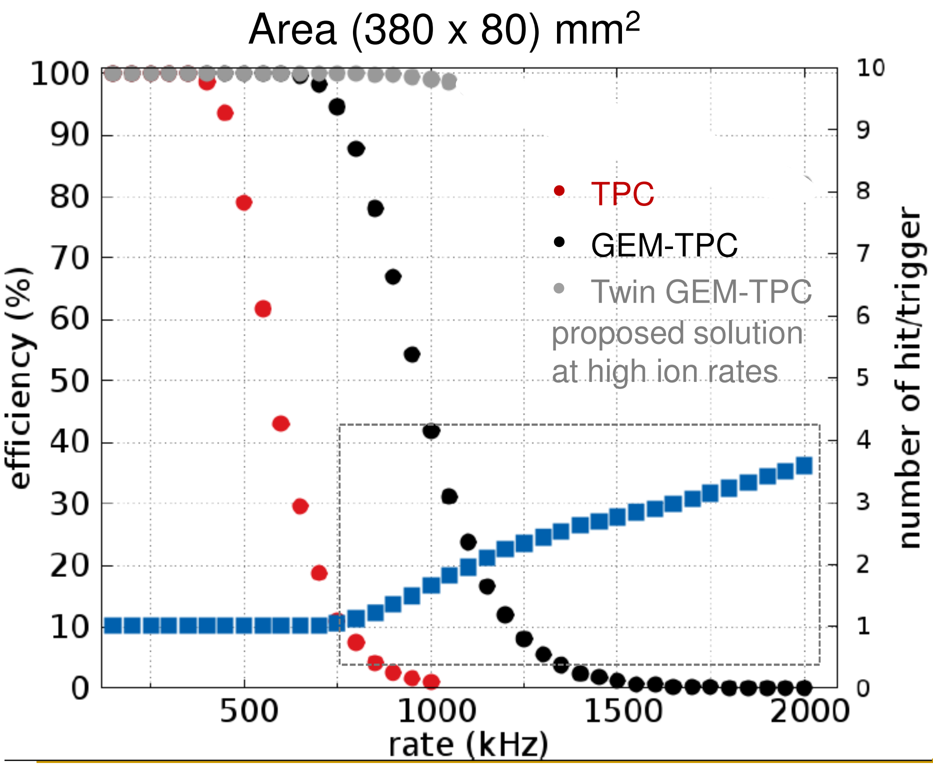

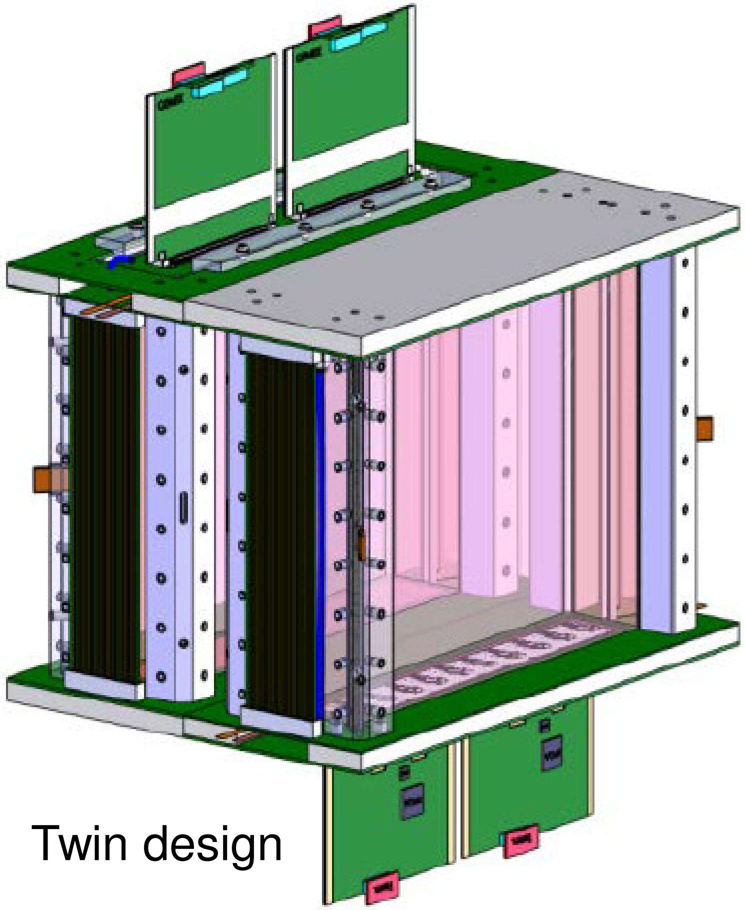

Twin design

Particle tracking at the Super-FRS

Gas detector based on GEM technology

- 32 units
- pos resolution σ <1 mm
- active area 380/200mm x 80/50mm
- max rate up to 10^7/spill
- high dynamic range (> 1000)
- multi-channel FEE → ASIC for time (and energy) measurements,
  link board to compress and multiplex data,
  zero suppression data,
  readout dead-time free 1-10 MHz

ΔE detector

Standard ΔE detector

A suitable ΔE detector needs to have

- good energy resolution
- high counting rate capability
- robustness against beam bombardment

Gas ionization chambers are

- extremely stable if equipped with gas flow system
- can provide energy resolution as good as that of semiconductor detectors
- large-scale detector easy to fabricate

⇩

Multi Sampling Ionization Chamber (MUSIC)

MUSIC detector

8 anode strips with 50 mm active length

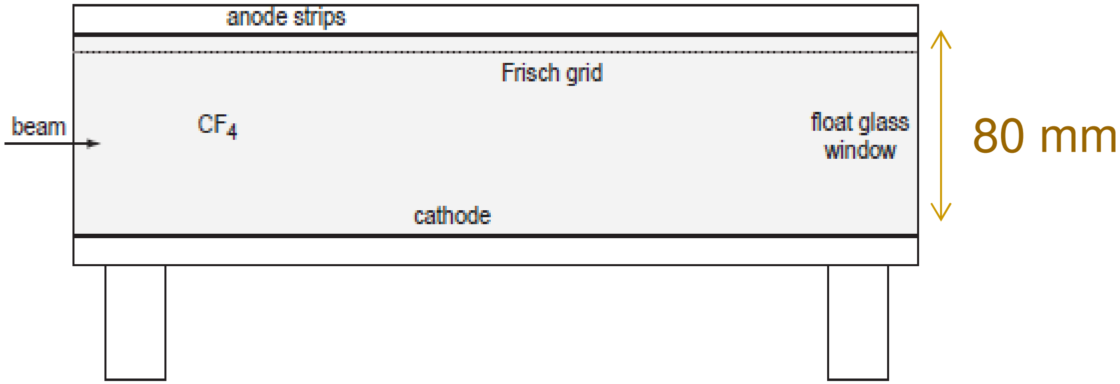

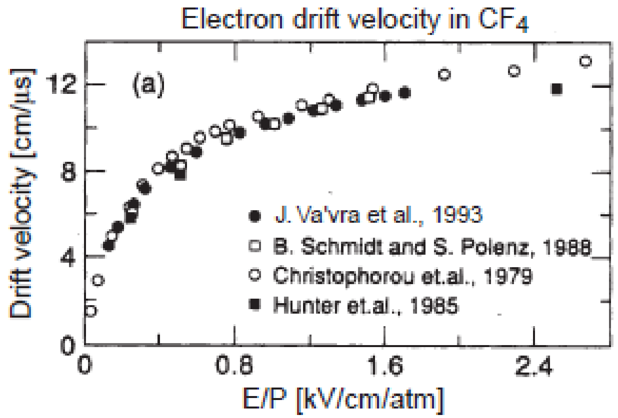

Tested successfully for particle rates of up to 200 kHz, thanks to a 10th order shaper which returns very fast to zero line and an overall DC-coupling is used, which avoids rate dependent baseline drift.

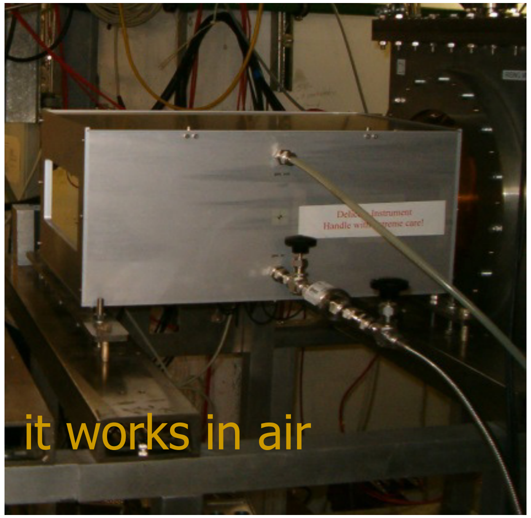

TU Munich

http://www-w2k.gsi.de/frs/technical/FRSsetup/detectors/music.asp

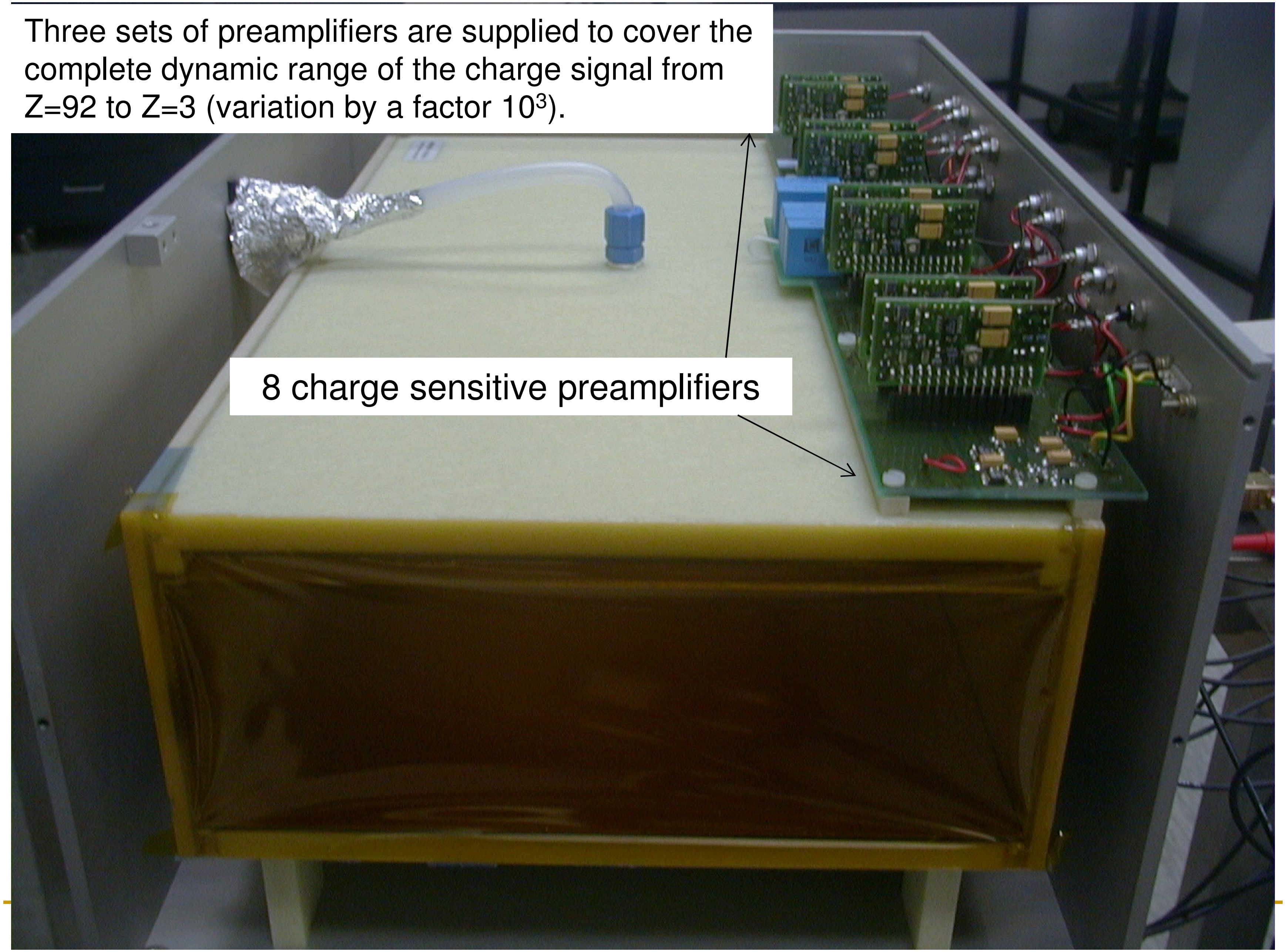
Three sets of preamplifiers are supplied to cover the complete dynamic range of the charge signal from Z=92 to Z=3 (variation by a factor 10^3).
8 charge sensitive preamplifiers

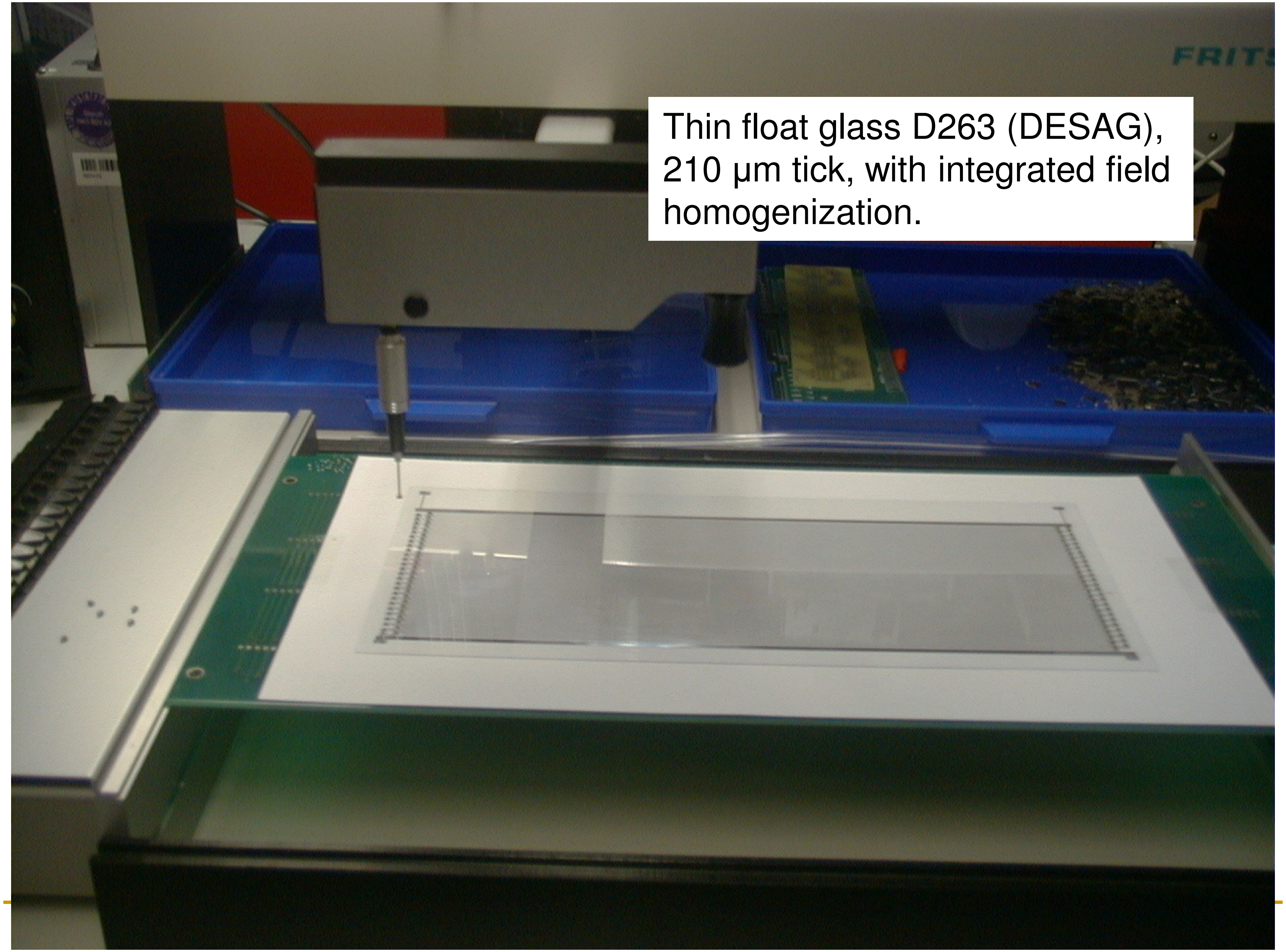

Thin float glass D263 (DESAG), 210 μm tick, with integrated field homogenization.

The field homogenization consists of Al strips (thickness 1 μm) deposited on the float glass by photolithography and a voltage divider with resistors glued directly onto the glass plate.

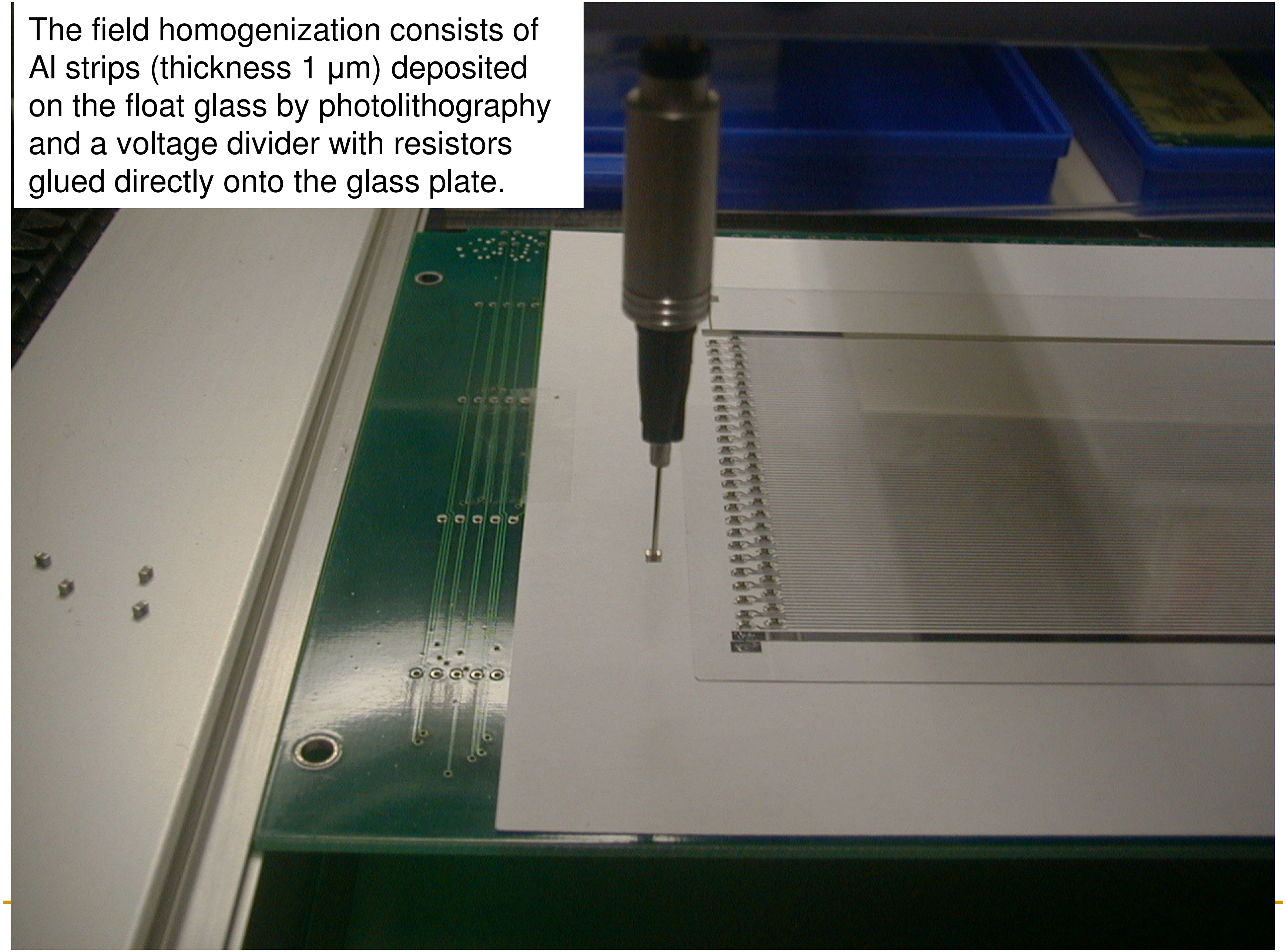

Count rate limit

... but they are not fast enough to resolve the signals of individual beam particles at intensity > 30-40 kHz.

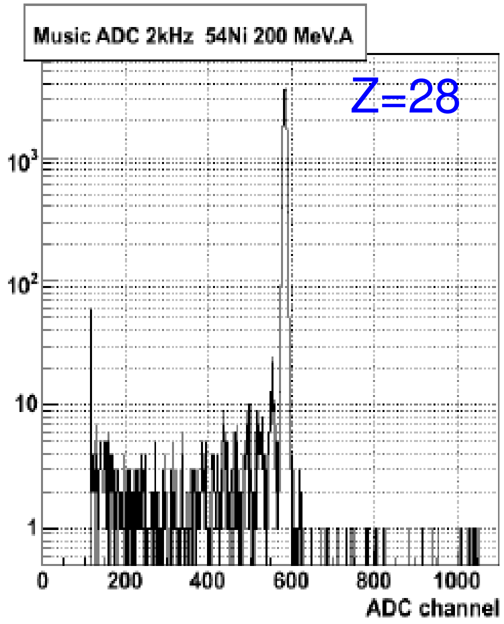

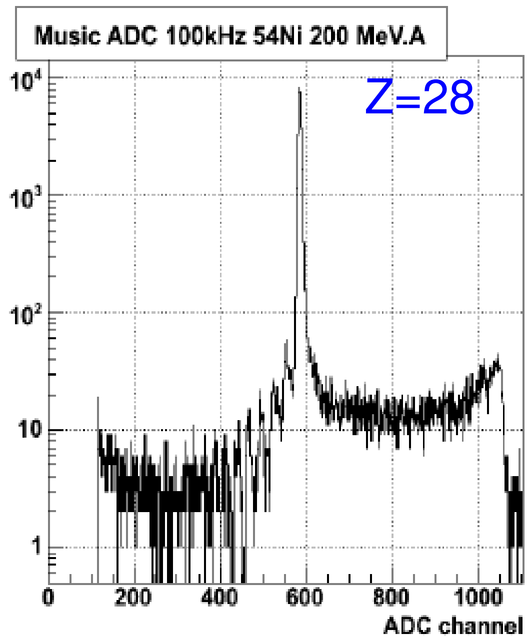

Pile-up in the MUSIC shaper output gives wrong Z identification.

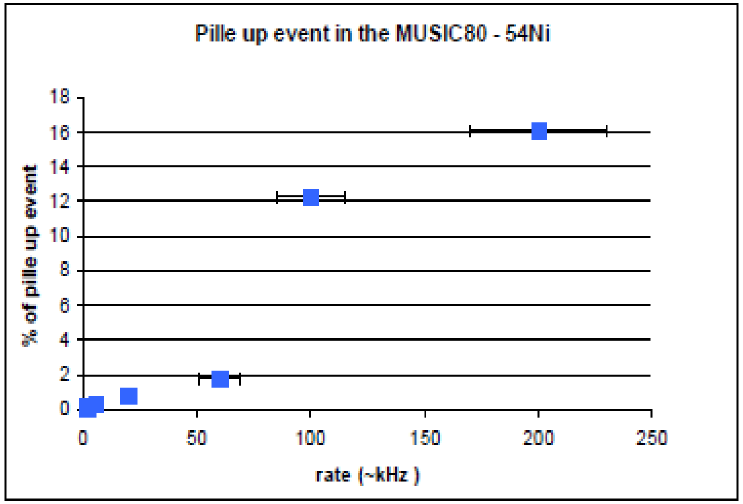

FEBEX readout

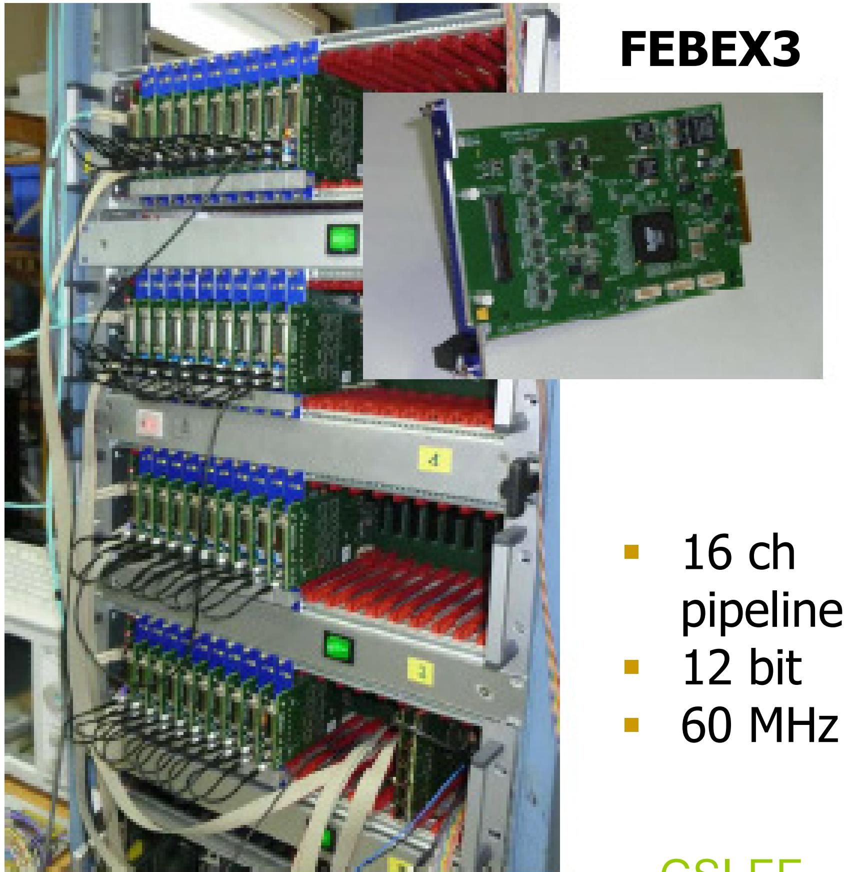

FEBEX3

- 16 ch pipeline ADC
- 12 bit
- 60 MHz clock

GSI-EE

Not only pile-up rejection ...
correct for pile-up effect is needed !

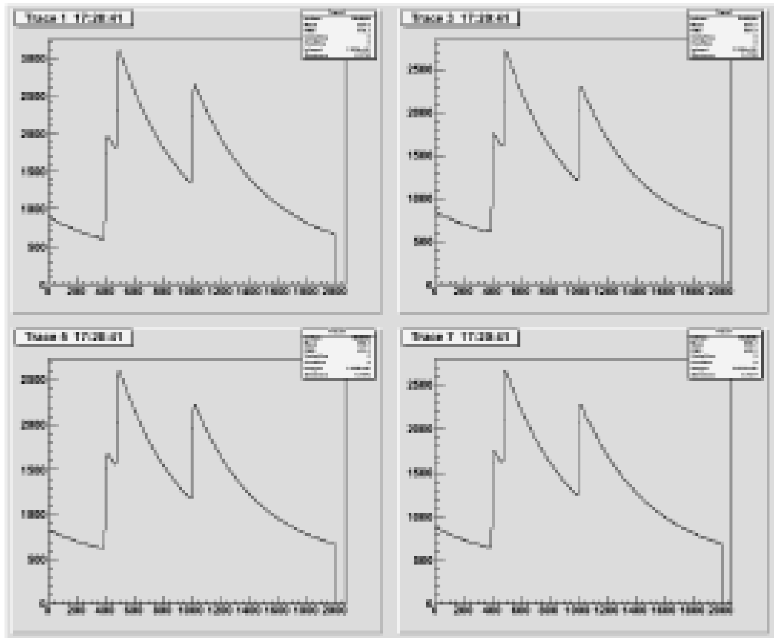

Toward higher counting rate

Design employing a stacked configuration of thin *grid-less* gas ionization chamber

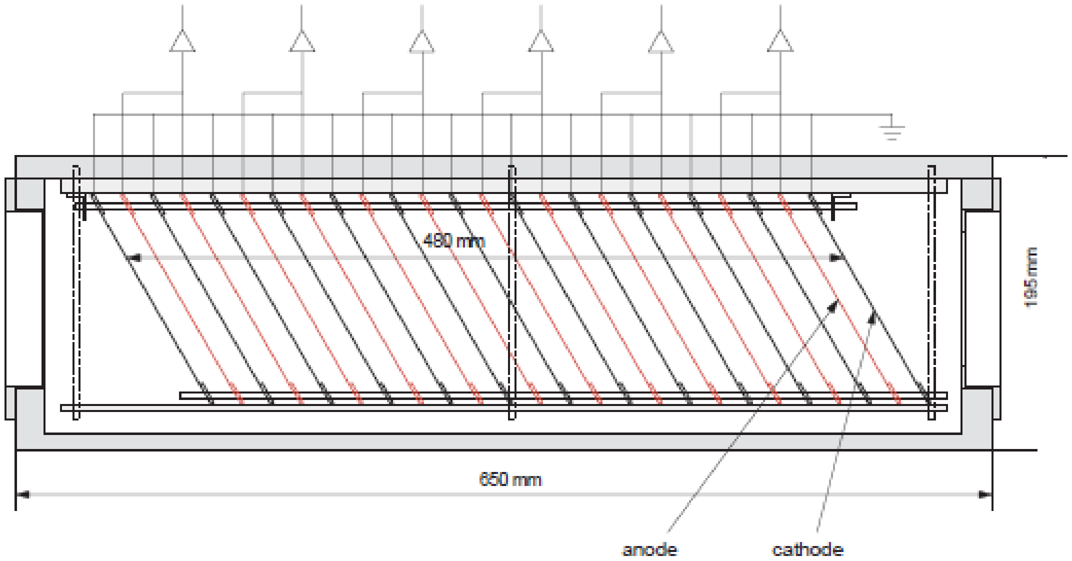

TEGIC

K. Kimura et al., *NIM A* 538 (2005) 608

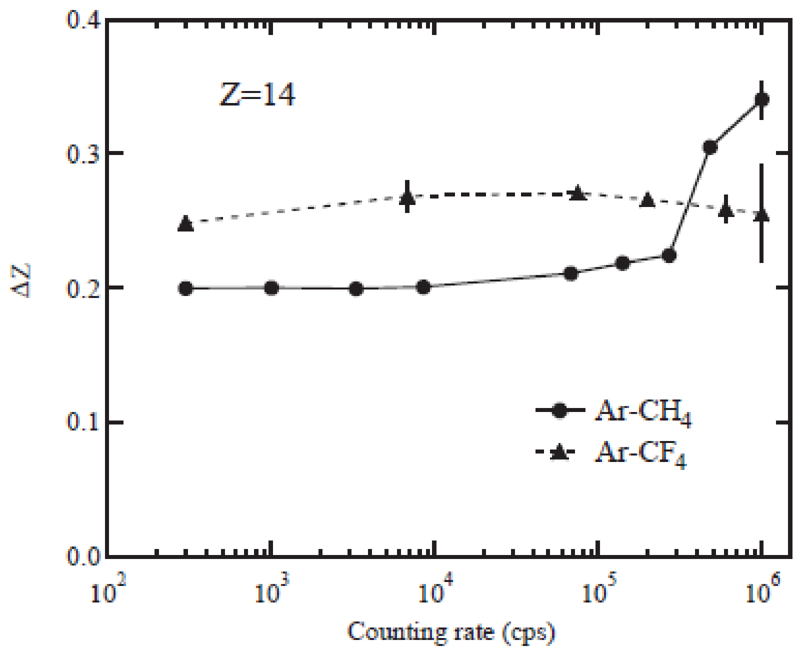

Electrodes plates **tilted** (30°) in order to avoid recombination

Bipolar shaping of anode signals

Velocity and Z dependence

A/Z=2

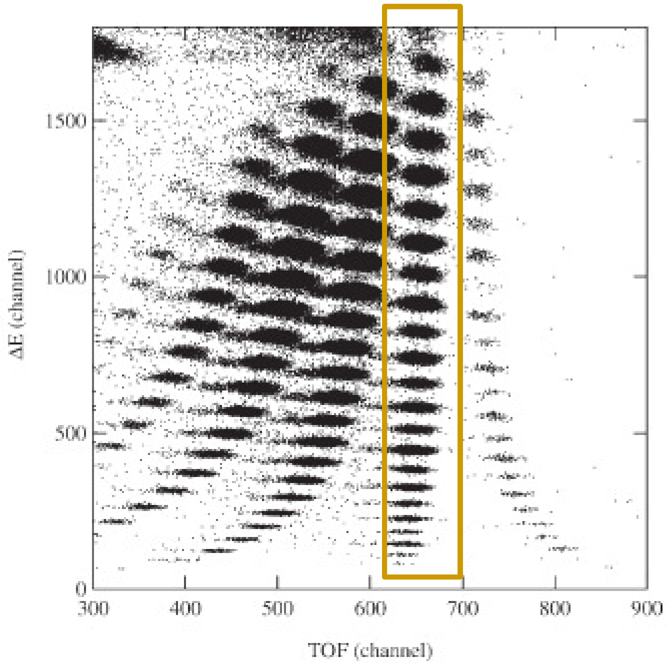

Fig. 2. Two-dimensional scatter plot of ΔE vs. TOF for the secondary beam produced by nuclear fragmentation of ^{56}Fe at 90 A MeV.

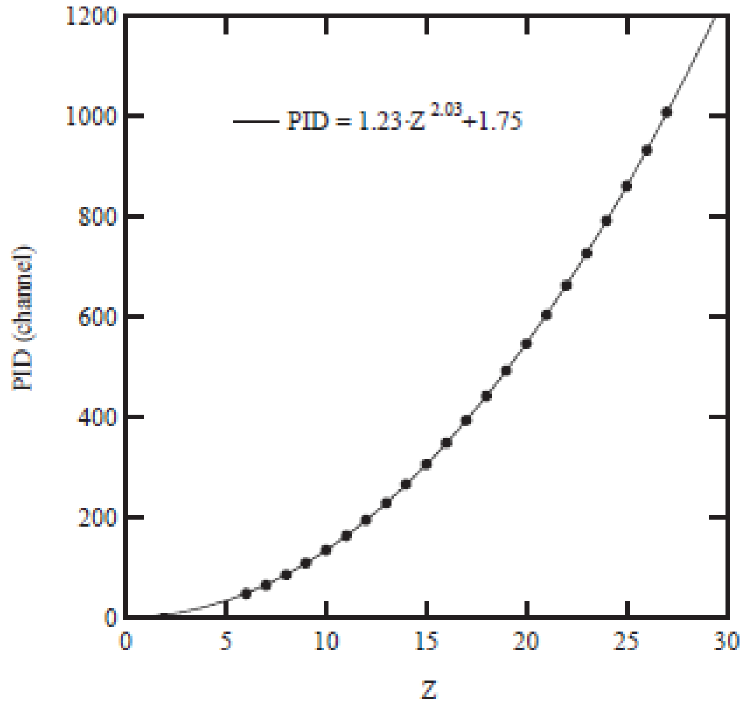

Fig. 4. PID vs. Z relationship for $A/Z = 2$ nuclides. A solid curve is the best fit to the PID and indicates that the PID is proportional to $Z^{2.03}$. The errors of the PID channels are less than the marker size.

K. Kimura et al., *NIM A* 538 (2005) 608

Comparison scCVD-DD and MUSIC

Be + ^{238}Xe @1GeV/u

scCVD -DD 4x4x0.4 mm^3

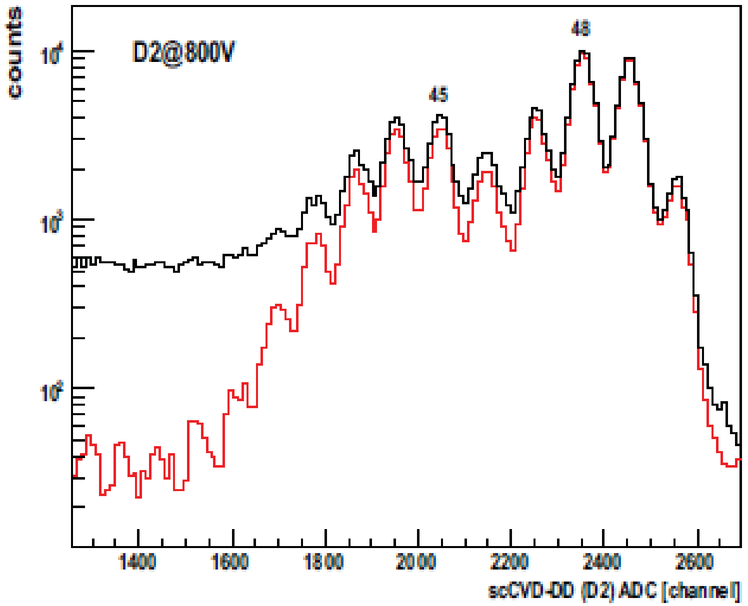

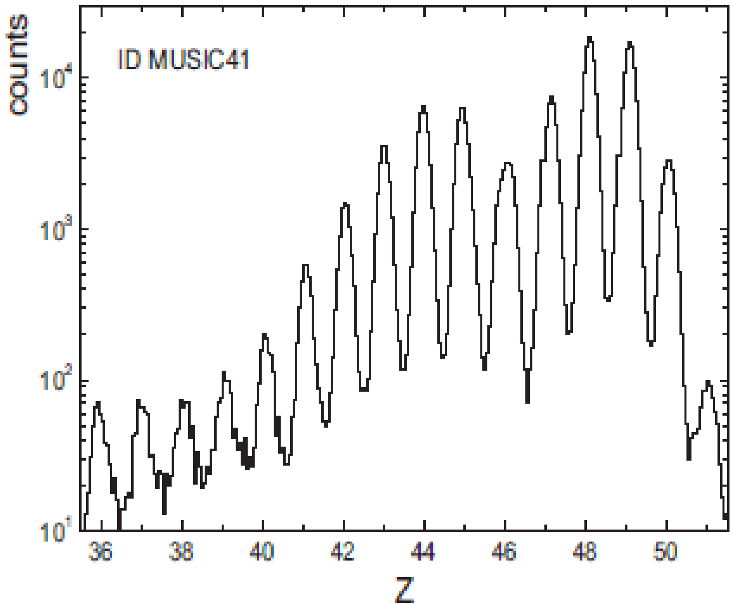

M. Pomorski, *PhD thesis* – Uni Frankfurt (2008)

Other PID detectors

Isomer TAGger (ITAG)

HPGe: mechanical cooling system,
mounted in a movable holder,
shielded with 50 mm Pb

2 Scintillators: 5 mm BC-400

Stopper: (150 x 150) mm^2 Al
thickness 4.2 mm

F. Farinon et al., *GSI report* 2009

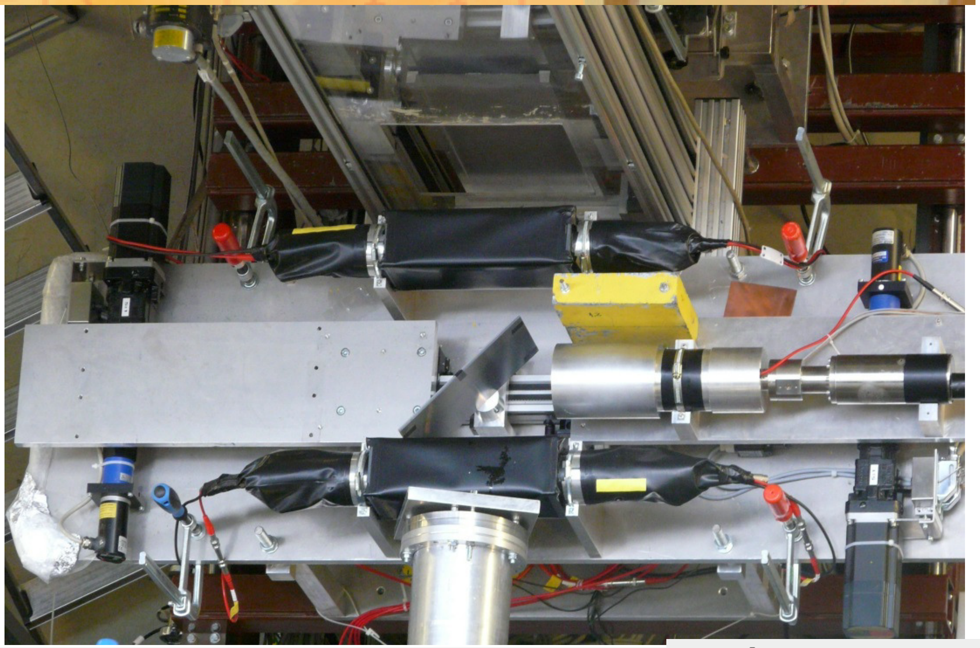

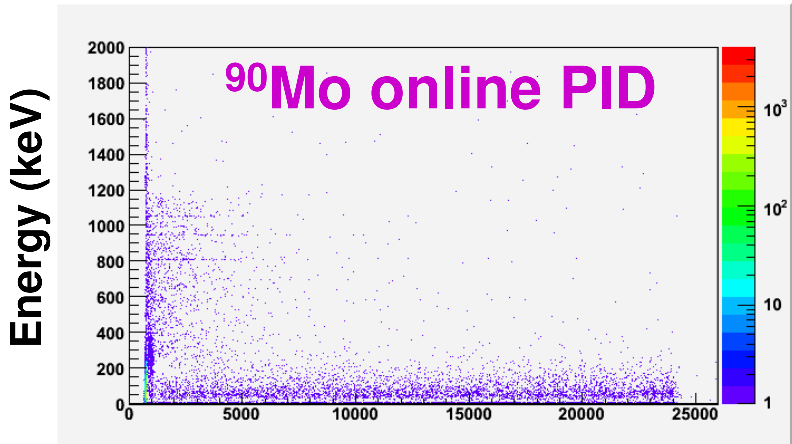

Time Sc41-Ge (ns)

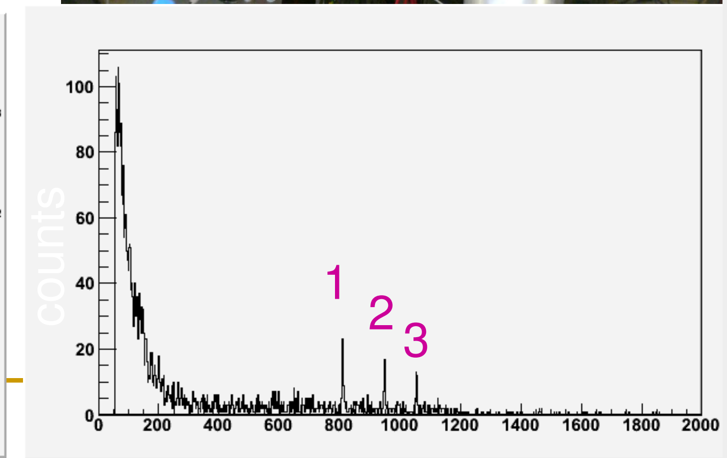

Energy (keV)

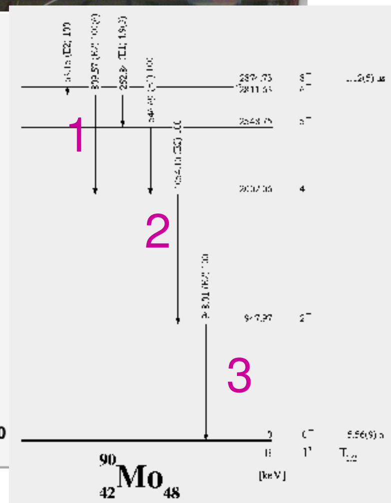

α tagger and stopping gas cell

Si active stopper : DSSSD by Microns,
16 x-strips, y-strips,
(50 x 50) mm^2,
1 mm thickness

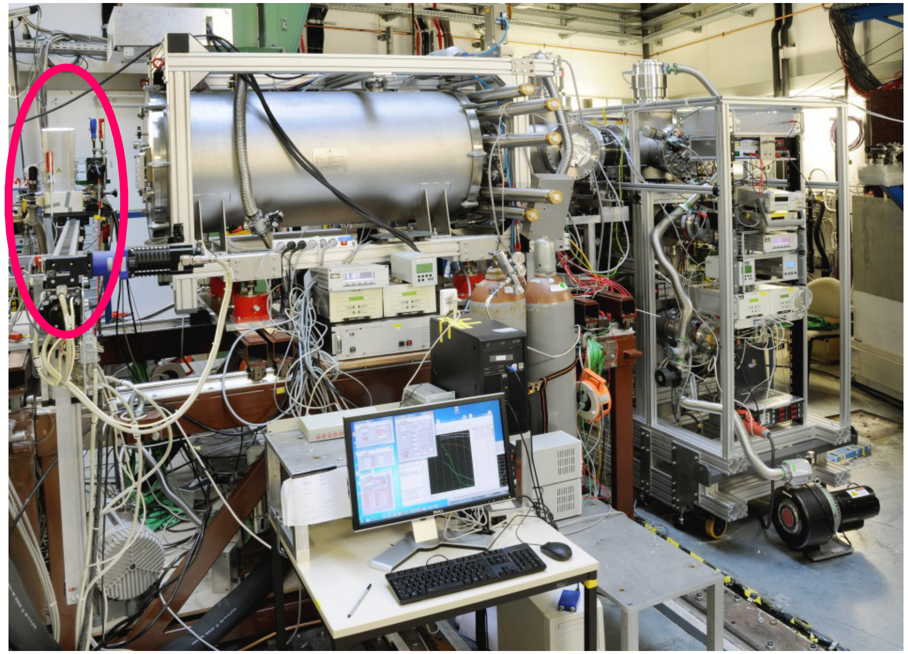

M. P. Reiter et al., *GSI report* 2012

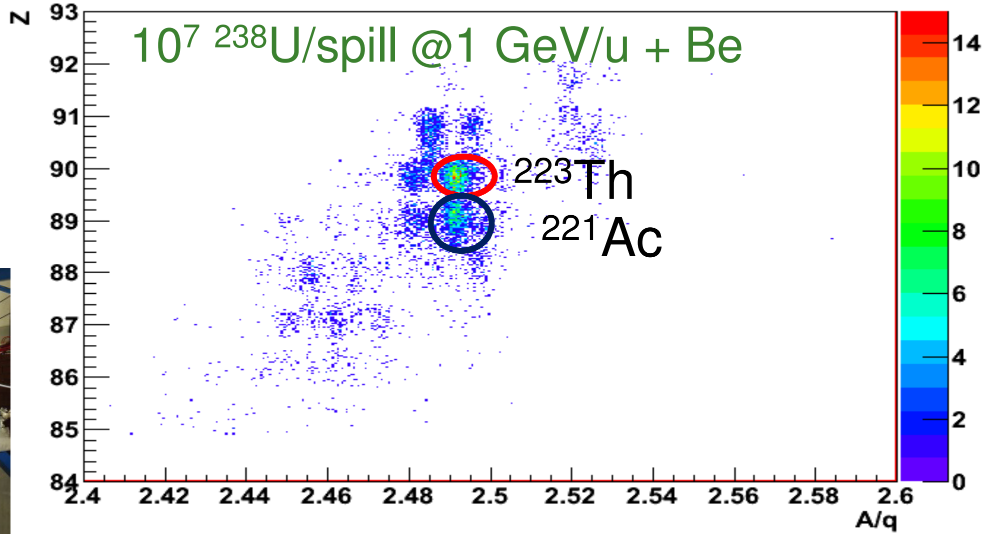

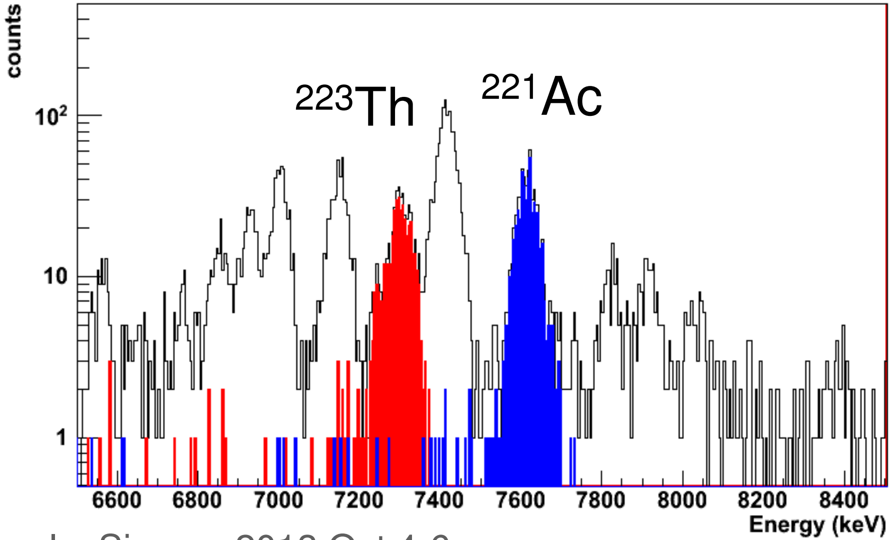

Energy Buncher requirements

- sufficient yield of the isotope of interest (10 to 10^4 ions/s)
- efficient stopping and extraction of relativistic projectile/fission fragments in a short time (<< 1 s) requires gas cell (it will erase all *memory* of Super-FRS beam, no direct dependence on the beam properties)
- but gas cell needs well separated beam (>1:10^3) otherwise too much ionization load from unwanted isotopes

Energy bunching is required

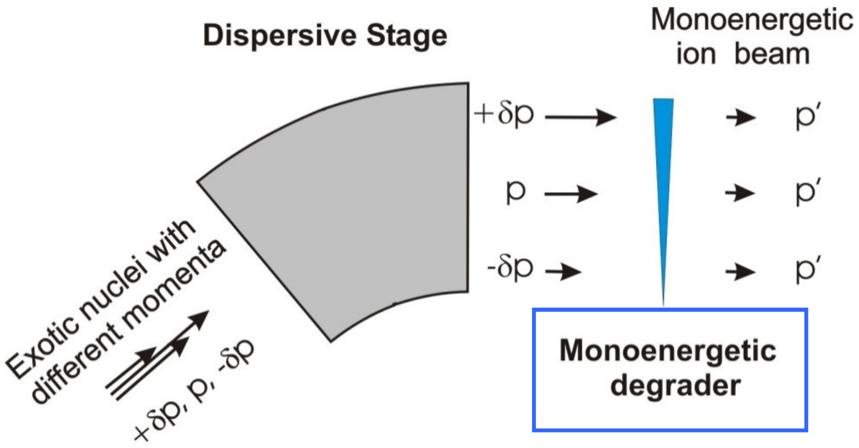

to keep the gas cell reasonably short and to assure good efficiency at reasonable pressures

α-decay half-lives

For understanding the r-process abundances of elements with **A > 210**, including the cosmochronometers U and Th, and for determining the end point of the rp-process.

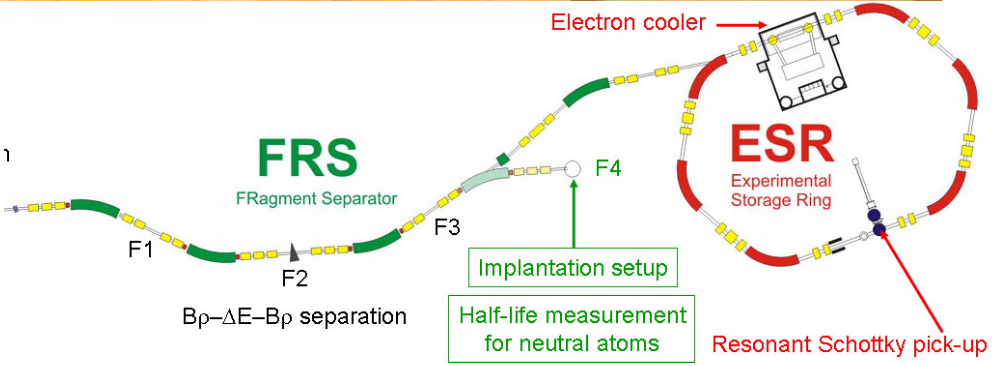

$T_{1/2}$ measurements:

- by implantation-decay technique @FRS-F4
- highly charged α-emitters at @FRS-ESR

^{214}Ra

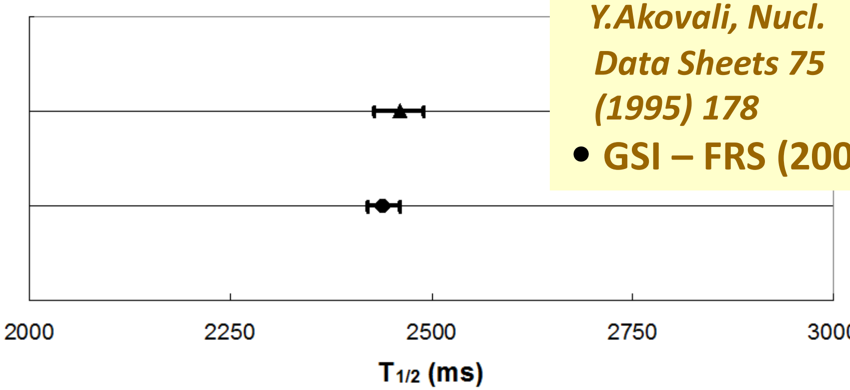

▲ Literature
Y.Akovali, Nucl. Data Sheets 75 (1995) 178
● GSI – FRS (2008)

^{213}Fr

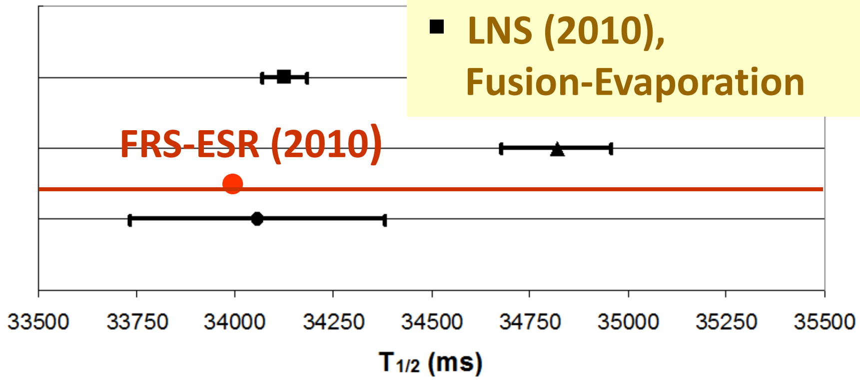

▲ Literature
M.S.Basunia, Nucl. Data Sheets 108 (2007) 658
● GSI – FRS (2008)
■ LNS (2010), Fusion-Evaporation

Time resolved Shottky spectrum

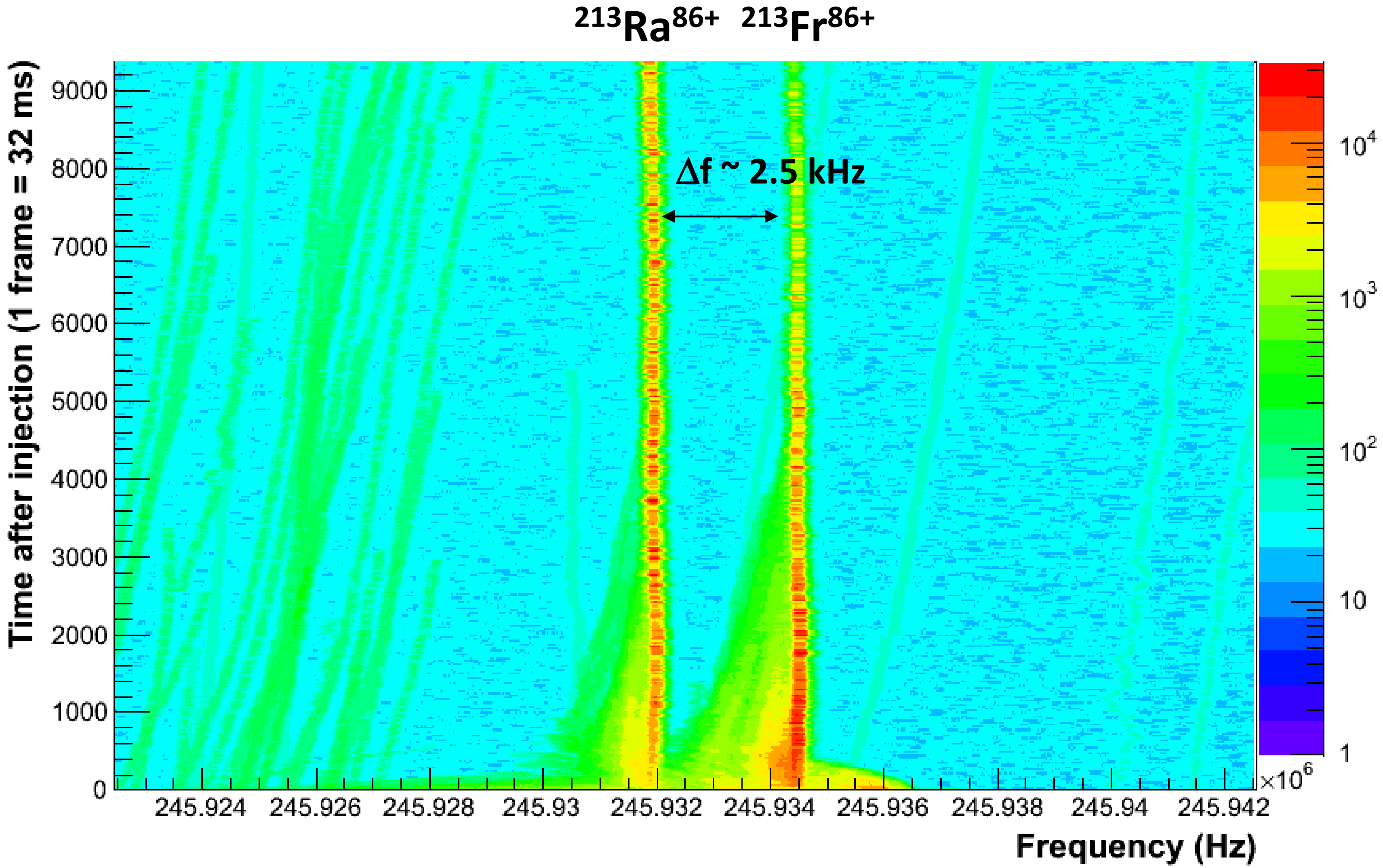

C. Nociforo et al. *Phys. Scr.* T150 (2012) 014028

^{213}Fr case: pilot experiment (July 2010)

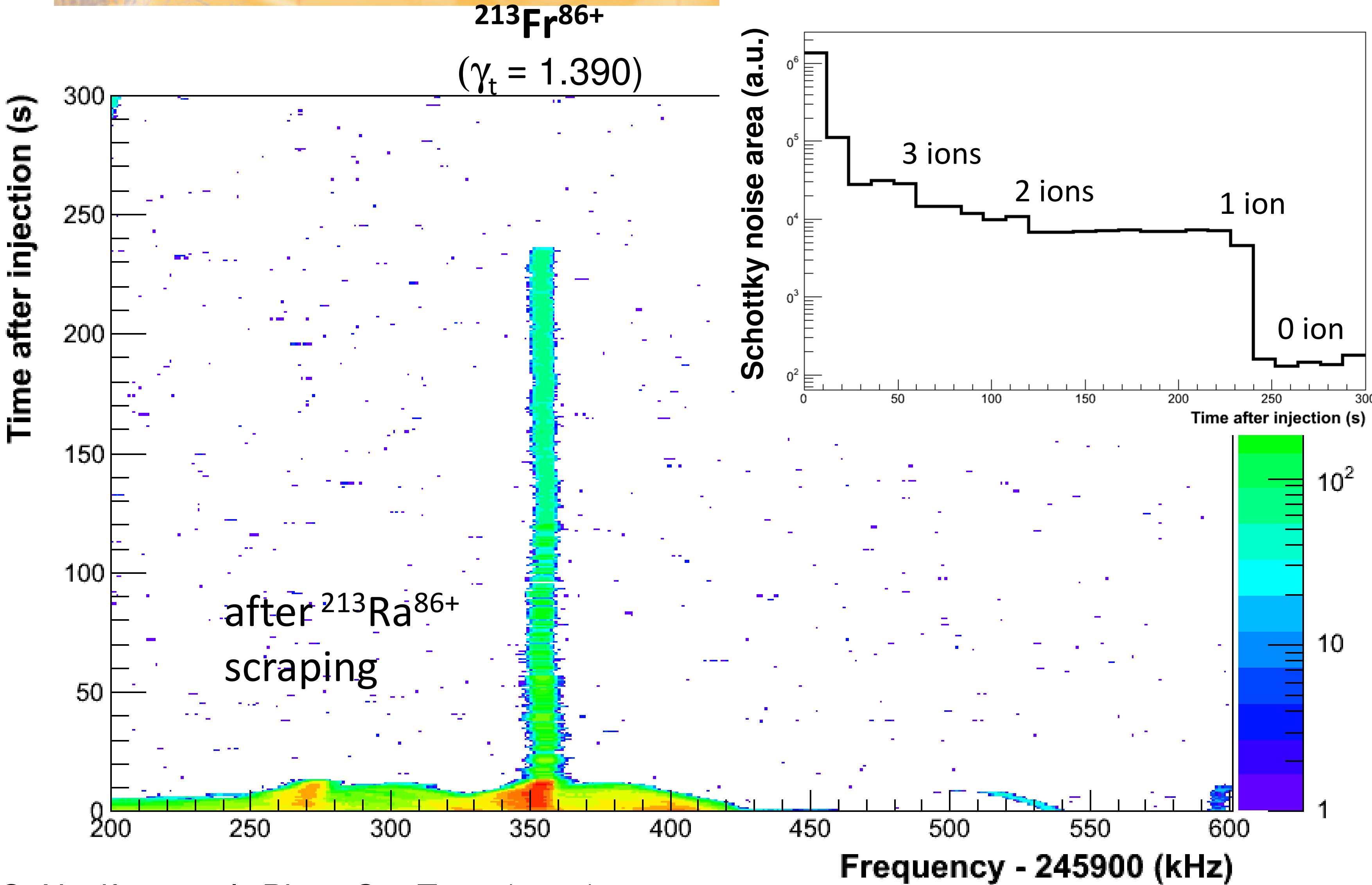

C. Nociforo et al. *Phys. Scr.* T150 (2012) 014028

Conclusions

- Overview of in-flight separation method of exotic beams

- The Super-FRS at FAIR and its PID detecting system:
  ToF , tracking and ΔE detectors

  - challenges: large area, high-rate capability, fast timing,
    large dynamic range, high resolution
  - prototype: GEM-TPC, diamond, Si
  - new FEE: GEMEX, PADI, FEBEX

Outlooks: beam test in 2014

The Super-FRS design is well suitable for nuclear experiments at the forefront of science.